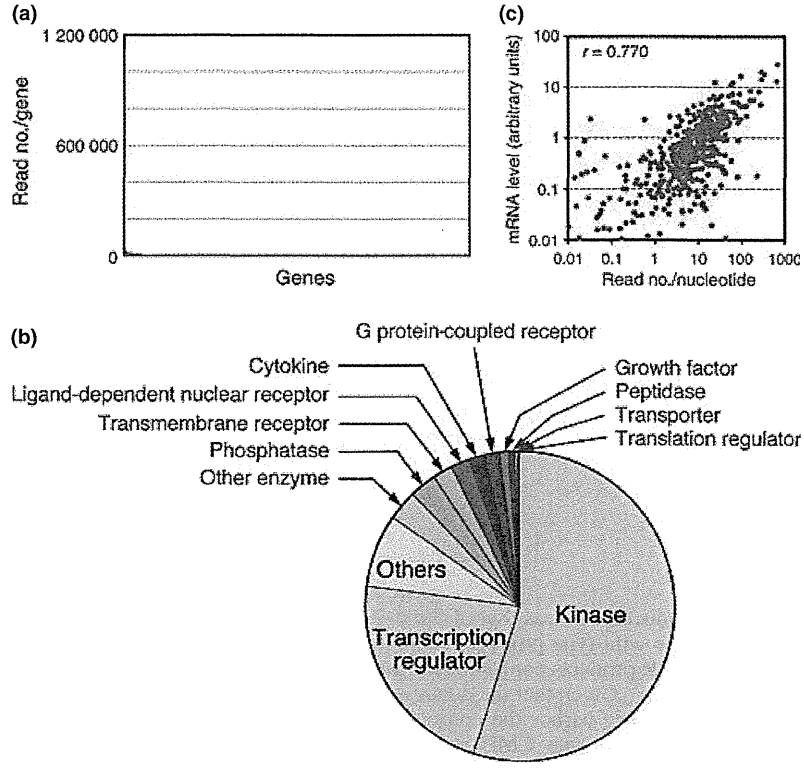

Fig. 2. Capture of a selected set of cDNA. (a) Read number for each gene was calculated from the sequencing data for the unselected cDNA of KCL-22-SR cells. Genes were sorted according to their read number. A small number of genes accounted for most of the sequence reads. (b) Functional annotation for the encoded proteins of our target cDNA (n = 913). (c) Read number per nucleotide for each captured cDNA in KCL-22-SR cells is compared with the expression intensity (arbitrary units) of the same cDNA examined with an HGU95Av2 microarray. Pearson's correlation coefficient (r) for the comparison is also demonstrated.

We therefore attempted to construct a custom SureSelect system to capture cDNA for cancer-related genes. For this purpose, we selected 913 genes that yielded 56 892 hybridization probes corresponding to ~3.77 Mbp of total capture capacity. The target genes encoded human protein kinases (all members in the human genome), transcription regulators, phosphatases, and other proteins (Fig. 2b; Table S1).

To compare the information provided by the sequence data from unselected and captured cDNA, we purified target cDNA from KCL-22-SR cells with the use of our custom SureSelect system, and determined their nucleotide sequences with GAIIx. A comparable amount of filter-passed reads (39.2 million) to that of unselected cDNA were thus obtained. We found that 88% of the captured cDNA were mapped to the target genes in our SureSelect system, while only 6.6% of the unselected cDNA were mapped to the 913 targets (data not shown). The read number obtained for each gene in the captured cDNA dataset is shown in Figure S2, with the distribution being markedly different from that obtained by sequencing of the unselected cDNA (Fig. 2a). As expected, the read number per nucleotide in each cDNA for the captured dataset was highly correlated to the expression intensity of the same gene quantified with the HGU95Av2 GeneChip expression array (Pearson's correlation coefficient = 0.770, $P < 2.2 \times 10^{-16}$) (Fig. 2c).

We further isolated target cDNA from other CML cell lines, including K562, KU812, MEG-01s, and NCO2, and the purified cDNA fragments were subjected to GAIIx sequencing. As in the case for KCL-22-SR, 86–88% of the obtained reads were successfully mapped to the target cDNA in each cell line (Table S2).

Screening of fusion cDNA. Our target set of 913 genes did not include *BCR*, but it did contain *ABL1*. Thus, if we were able to isolate sequence reads encompassing the fusion point of *BCR–ABL1*, cDNA-capture approaches for a given gene set would likely be able to detect gene fusions to unknown partners. In fact, we detected 45 sequence reads for KCL-22-SR cells that covered the *BCR–ABL1* fusion point (Fig. 3a). Likewise, the sequence datasets for K562, KU812, MEG-01s, and NCO2 cells contained 53, 8, 11, and 10 such fusion reads, respectively (data not shown). Furthermore, our sequence data faithfully recapitulated two variants of *BCR–ABL1* cDNA in these cell lines; a fusion variant between exon 13 of *BCR* and exon 2 of *ABL1* was detected in KCL-22-SR, MEG-01s, and NCO2 cells, whereas a fusion variant between exon 14 of *BCR* and exon 2 of *ABL1* was detected in K562 and KU812 cells.[14]

In addition to *BCR–ABL1*, we identified 72 independent candidates for fusion cDNA (including fusions to non-coding RNA) from the CML cell lines. Surprisingly, however, the screening of fusion genes among the unselected cDNA of KCL-22-SR with our rather non-stringent threshold (≥4 reads mapped to a candidate fusion point) failed to isolate *BCR–ABL1* cDNA. We could not even detect any fusion candidates (involving one of our target genes in either or both ends of fusion events) from this dataset, while a total of nine candidates (including *BCR–ABL1*) were isolated from the captured cDNA of the same cell line.

Our Bowtie mapping of both ends of each read to human mRNA or genome databases (Fig. S1) resulted in the detection of not only *BCR–ABL1* fusions, but also a large number of alternatively-spliced messages. From the captured cDNA of KCL-22-SR, for instance, we could detect 79 alternatively-spliced transcripts for 72 independent genes (data not shown). In contrast, from the unselected cDNA of the same cell line, only three independent, alternatively-spliced transcripts were identified among three genes within the 913 targets.

One such example of alternatively-spliced message was *MLL* (ensemble accession no.: ENST00000389506) in KU812, MEG-01s, and K562 cells. In addition to a set of reads that completely matched exon 3 of *MLL*, we obtained reads that lacked an internal 2193-bp sequence in exon 3 (Fig. 3b). Such in-frame truncation would be expected to generate an MLL protein lacking amino acids 276–1006 of the wild-type protein. To confirm the presence of such transcripts, we performed RT–PCR analysis with total RNA from KU812 cells, and PCR primers designed as in Figure 3b. The combination of the F-1 and R primers would be expected to yield both the wild-type (2536 bp) and truncated

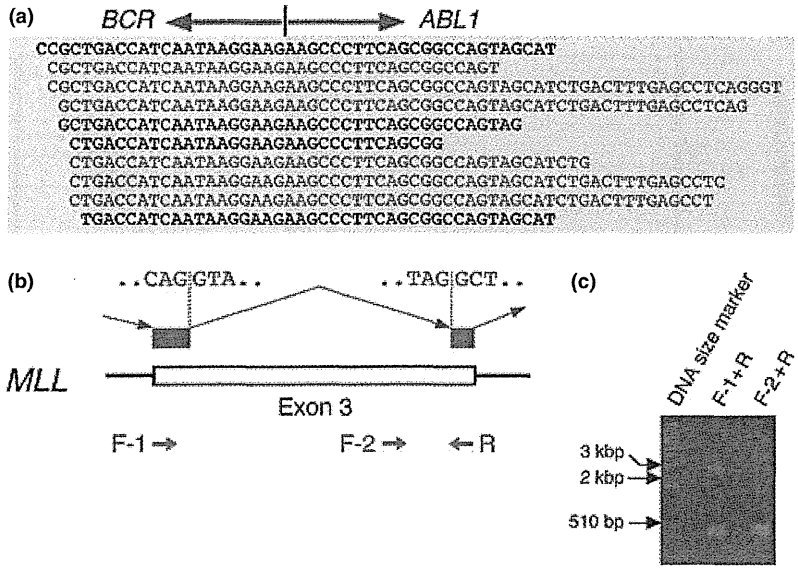

Fig. 3. Detection of gene fusions and alternative mRNA splicing in CML cells. (a) Our computational pipeline yielded 45 reads for KCL-22-SR cells that encompassed the fusion point of breakpoint cluster region (*BCR*)-Abelson murine leukemia viral oncogene homolog 1 (*ABL1*) cDNA, some of which are shown aligned. Reads in the sense or antisense strand are designated in black and blue letters, respectively, and the *BCR* and *ABL1* portions of the sequences are shaded differentially. (b) Some of the reads that mapped to exon 3 of mixed-lineage leukemia (*MLL*) skipped a 2193-bp region within this exon. Nucleotide sequences of the cryptic splicing sites are shown, as are the positions of PCR primers used to confirm the alternative splicing. (c) Gel electrophoresis of the RT–PCR products obtained with total RNA isolated from KU812 cells and with either the F-1 and R primer pair or the F-2 and R primer pair. A 1-kb ladder of DNA size markers was also included.

(343 bp) products, whereas that of the F-2 and R primers would yield only the wild-type product of 339 bp. Gel electrophoresis of the RT–PCR products confirmed the presence of the truncated mRNA (Fig. 3c). Given that the donor and acceptor sites for this alternative splicing harbor the consensus sequences for mRNA splicing (Fig. 3b), some CML cells likely make use of such cryptic splicing sites after *MLL* transcription.

Other variants. From the captured cDNA for KCL-22-SR, NCO2, MEG-01s, K562, and KU812 cells, we detected 156, 18, 28, 23, and 21 non-synonymous mutations among the 913 target genes, respectively. An analysis of the unselected cDNA from KCL-22-SR, however, identified only 19 mutations within the target genes, 16 of which were discovered in the captured cDNA as well. Comparison of the read sequences from the unselected KCL-22-SR cDNA to all RefSeq exonic sequences discovered a total of 597 non-synonymous mutations.

Furthermore, 19, eight, four, 11, and two indels were detected with the captured cDNA of KCL-22-SR, NCO2, MEG-01s, K562, and KU812, respectively. Most of the detected indels were only 1 bp in length, whereas the others were either 2 or 3 bp (Fig. S3). Detailed analysis of these nucleotide changes will be described elsewhere (Toshihide Ueno and Yoshihiro Yamashita, personal communication).

One of the most frequent genetic changes in the blast crisis of CML is point mutation or loss (or both) of *TP53*.[21] Indeed, our sequence data for this gene revealed non-synonymous point mutations in NCO2 and KU812 cells, a 1-bp insertion in K562 cells, a 1-bp deletion in KCL-22-SR cells, and a 3-bp deletion in MEG-01s cells (Fig. 4; Fig. S4; Table S3), all of which were confirmed by Sanger sequencing (data not shown). In NCO2 cells, for instance, 100% of *TP53* reads harbored a G-to-C substitution at nucleotide position 993 of *TP53* mRNA (GenBank accession no.: NM_000546), resulting in a glycine-to-arginine amino acid change (Fig. 4a). The data were also indicative of loss of heterozygosity for *TP53* in NCO2 cells. Similarly, 75% or 78% of *TP53* reads contained a C insertion or a CAC deletion in K562 (Fig. 4b) or MEG-01s (Fig. S4) cells, respectively.

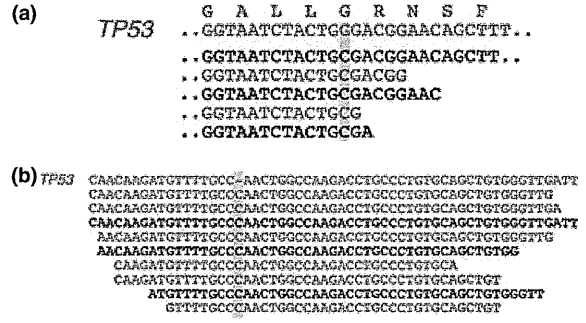

Fig. 4. Anomalies in *TP53* in CML cell lines. (a) Read sequences for NCO2 cells are shown aligned with the reference nucleotide and predicted amino acid sequences (red letters) for *TP53*, revealing a G-to-C substitution in all the reads. Sense or antisense strands are denoted in black and blue letters, respectively. (b) Alignment of the read sequences for K562 cells with the cDNA sequence of *TP53* as in (a), revealing a C insertion.

Discussion

We have shown that a cDNA-capture system, coupled with massively parallel sequencing, is a feasible and relatively simple approach to the simultaneous detection of point mutations, indels, and gene fusions in target cDNA. There are, however, both advantages and disadvantages of this technique compared with the conventional exon-capture system for genomic DNA.

The ability to detect gene fusions, in addition to other mutations with a single sequencing reaction, is one of the most important benefits of the cDNA-capture approach. Furthermore, the efficiency of exon capture with genomic DNA is dependent on the sequence context of each exon. The mean exon size for the human genome is only <200 bp, and the efficiency of exon purification is markedly affected by GC content and sequence complexity.[22] In contrast, even exons with a high GC content might be well isolated by the cDNA-capture system if adjacent exons have a normal GC content and are efficiently targeted by hybridization probes.

Levin *et al.*[20] conducted deep sequencing of captured cDNA for K562 cells, and identified five candidates for fusion genes in addition to *BCR–ABL1*. However, we could not detect any of the five candidates through our analysis with K562, probably because our 913 target genes did not contain those involved in the gene fusions in their report, other than nascent polypeptide-associated complex alpha subunit (*NACA*). While Levin *et al.* discovered primase, DNA, polypeptide 1 (*PRIM1*)–*NACA* fusion transcripts, the low expression level of *PRIM1–NACA* in K562 (only 2.5% of that of *BCR–ABL1* in their dataset)[20] might account for the failure in our analysis.

doi: 10.1111/j.1349-7006.2011.02105.x

However, for experiments based on capture of genomic DNA, sequencing a paired normal specimen allows the efficient subtraction of rare SNP not present in the current databases from the dataset of cancer tissue. This is not always the case, however, for the cDNA-capture approach, given that gene expression profiles differ markedly among samples (even among those obtained from the same individual). Genes with sequence alterations in the cancer specimen might not be expressed in a given normal specimen, and it is not possible to readily determine whether such alterations are germ-line polymorphisms, while algorithms to predict the effect on protein functions for a given amino acid change are currently available[23] and synonymous-to-non-synonymous ratio of nucleotide alterations for a given gene/dataset might provide clues as to how such changes are selected in tumor cells.[24]

In addition, the cDNA-capture system cannot obtain a sufficient number of reads for genes expressed at a low level, and the overall sensitivity of cDNA capture is dependent on the total read number provided by sequencers. We are able to run only two samples per flow cell of the GAIIx system, whereas up to eight samples can be run in a single flow cell for whole exome sequencing of human genomic DNA.

Despite such limitations, our study shows that cDNA capture is an efficient process, and extensive sequencing of such purified cDNA is a straightforward approach to interrogate the target cDNA for various genetic changes in a single platform. Large-scale resequencing of hundreds of cancer specimens might thus become within the scope of private laboratories with the adoption of the cDNA-capture approach.

Acknowledgments

This study was supported in part by grants for Research on Human Genome Tailor-Made and for Third-Term Comprehensive Control Research for Cancer from the Ministry of Health, Labor, and Welfare of Japan; Grants-in-Aid for Scientific Research (B) and for Young Scientists (A) from the Ministry of Education, Culture, Sports, Science, and Technology of Japan; and by grants from the Japan Society for the Promotion of Science, Takeda Science Foundation, the Naito Foundation, Sankyo Foundation of Life Science, The Sagawa Foundation for Promotion of Cancer Research, the Yasuda Medical Foundation, the Mitsubishi Foundation, and Kobayashi Foundation for Cancer Research.

Disclosure Statement

K. Fukumura, M. Ando, M. Kawazu, Y.L. Choi and H. Mano belong to the Department of Medical Genomics, Graduate School of Medicine, University of Tokyo, which receives research funding from Illumina Inc.

References

1 Stratton MR, Campbell PJ, Futreal PA. The cancer genome. *Nature* 2009; **458**: 719–24.
2 Mardis ER. A decade's perspective on DNA sequencing technology. *Nature* 2011; **470**: 198–203.
3 Ledford H. Big science: the cancer genome challenge. *Nature* 2010; **464**: 972–4.
4 Pleasance ED, Cheetham RK, Stephens PJ *et al.* A comprehensive catalogue of somatic mutations from a human cancer genome. *Nature* 2010; **463**: 191–6.
5 Ley TJ, Mardis ER, Ding L *et al.* DNA sequencing of a cytogenetically normal acute myeloid leukaemia genome. *Nature* 2008; **456**: 66–72.
6 Totoki Y, Tatsuno K, Yamamoto S *et al.* High-resolution characterization of a hepatocellular carcinoma genome. *Nat Genet* 2011; **43**: 464–9.
7 Wei X, Walia V, Lin JC *et al.* Exome sequencing identifies GRIN2A as frequently mutated in melanoma. *Nat Genet* 2011; **43**: 442–6.
8 Otto EA, Hurd TW, Airik R *et al.* Candidate exome capture identifies mutation of SDCCAG8 as the cause of a retinal-renal ciliopathy. *Nat Genet* 2010; **42**: 840–50.
9 Bilguvar K, Ozturk AK, Louvi A *et al.* Whole-exome sequencing identifies recessive WDR62 mutations in severe brain malformations. *Nature* 2010; **467**: 207–10.
10 Mitelman F. Recurrent chromosome aberrations in cancer. *Mutat Res* 2000; **462**: 247–53.
11 Soda M, Choi YL, Enomoto M *et al.* Identification of the transforming *EML4–ALK* fusion gene in non-small-cell lung cancer. *Nature* 2007; **448**: 561–6.
12 Tomlins SA, Rhodes DR, Perner S *et al.* Recurrent fusion of TMPRSS2 and ETS transcription factor genes in prostate cancer. *Science* 2005; **310**: 644–8.
13 Ohmine K, Nagai T, Tarumoto T *et al.* Analysis of gene expression profiles in an imatinib-resistant cell line, KCL22/SR. *Stem Cells* 2003; **21**: 315–21.
14 Drexler HG, MacLeod RA, Uphoff CC. Leukemia cell lines: *in vitro* models for the study of Philadelphia chromosome-positive leukemia. *Leuk Res* 1999; **23**: 207–15.
15 Choi YL, Tsukasaki K, O'Neill MC *et al.* A genomic analysis of adult T-cell leukemia. *Oncogene* 2007; **26**: 1245–55.
16 Langmead B, Trapnell C, Pop M, Salzberg SL. Ultrafast and memory-efficient alignment of short DNA sequences to the human genome. *Genome Biol* 2009; **10**: R25.
17 Altschul SF, Gish W, Miller W, Myers EW, Lipman DJ. Basic local alignment search tool. *J Mol Biol* 1990; **215**: 403–10.
18 Li H, Durbin R. Fast and accurate short read alignment with Burrows–Wheeler transform. *Bioinformatics* 2009; **25**: 1754–60.
19 Fujita PA, Rhead B, Zweig AS *et al.* The UCSC Genome Browser database: update 2011. *Nucleic Acids Res* 2011; **39**: D876–82.
20 Levin JZ, Berger MF, Adiconis X *et al.* Targeted next-generation sequencing of a cancer transcriptome enhances detection of sequence variants and novel fusion transcripts. *Genome Biol* 2009; **10**: R115.
21 Calabretta B, Perrotti D. The biology of CML blast crisis. *Blood* 2004; **103**: 4010–22.
22 Shen P, Wang W, Krishnakumar S *et al.* High-quality DNA sequence capture of 524 disease candidate genes. *Proc Natl Acad Sci USA* 2011; **108**: 6549–54.
23 Adzhubei IA, Schmidt S, Peshkin L *et al.* A method and server for predicting damaging missense mutations. *Nat Methods* 2010; **7**: 248–9.
24 Babenko VN, Basu MK, Kondrashov FA, Rogozin IB, Koonin EV. Signs of positive selection of somatic mutations in human cancers detected by EST sequence analysis. *BMC Cancer* 2006; **6**: 36.

Supporting Information

Additional Supporting Information may be found in the online version of this article:

Fig. S1. Algorithm of the computational pipeline.

Fig. S2. Read number distribution of all poly(A)-RNA data.

Fig. S3. Numbers of 1-, 2-, or 3-bp indels for the entire dataset.

Fig. S4. A CAG-deletion in the *TP53* message in MEG-01s cells.

Table S1. Gene list for the custom cDNA-capture system.

Table S2. Purification of the target cDNA in CML cell lines.

Table S3. TP53 mutation status in CML cell lines.

Please note: Wiley-Blackwell are not responsible for the content or functionality of any supporting materials supplied by the authors. Any queries (other than missing material) should be directed to the corresponding author for the article.

OPEN ACCESS Freely available online

PLoS one

KLC1-ALK: A Novel Fusion in Lung Cancer Identified Using a Formalin-Fixed Paraffin-Embedded Tissue Only

Yuki Togashi[1,2], Manabu Soda[3], Seiji Sakata[1], Emiko Sugawara[1,4], Satoko Hatano[1,2], Reimi Asaka[1,2], Takashi Nakajima[5], Hiroyuki Mano[3,6], Kengo Takeuchi[1,2]*

1 Pathology Project for Molecular Targets, The Cancer Institute, Japanese Foundation for Cancer Research, Tokyo, Japan, **2** Division of Pathology, The Cancer Institute, Japanese Foundation for Cancer Research, Tokyo, Japan, **3** Division of Functional Genomics, Jichi Medical University, Tochigi, Japan, **4** Department of Comprehensive Pathology, Graduate School, Tokyo Medical and Dental University, Tokyo, Japan, **5** Division of Diagnostic Pathology, Shizuoka Cancer Center, Nagaizumi, Shizuoka, Japan, **6** Department of Medical Genomics, Graduate School of Medicine, University of Tokyo, Tokyo, Japan

Abstract

The promising results of anaplastic lymphoma kinase (ALK) inhibitors have changed the significance of ALK fusions in several types of cancer. These fusions are no longer mere research targets or diagnostic markers, but they are now directly linked to the therapeutic benefit of patients. However, most available tumor tissues in clinical settings are formalin-fixed and paraffin-embedded (FFPE), and this significantly limits detailed genetic studies in many clinical cases. Although recent technical improvements have allowed the analysis of some known mutations in FFPE tissues, identifying unknown fusion genes by using only FFPE tissues remains difficult. We developed a 5′-rapid amplification of cDNA ends-based system optimized for FFPE tissues and evaluated this system on a lung cancer tissue with *ALK* rearrangement and without the 2 known ALK fusions EML4-ALK and KIF5B-ALK. With this system, we successfully identified a novel ALK fusion, KLC1-ALK. The result was confirmed by reverse transcription-polymerase chain reaction and fluorescence *in situ* hybridization. Then, we synthesized the putative full-length cDNA of *KLC1-ALK* and demonstrated the transforming potential of the fusion kinase with assays using mouse 3T3 cells. To the best of our knowledge, KLC1-ALK is the first novel oncogenic fusion identified using only FFPE tissues. This finding will broaden the potential value of archival FFPE tissues and provide further biological and clinical insights into ALK-positive lung cancer.

Citation: Togashi Y, Soda M, Sakata S, Sugawara E, Hatano S, et al. (2012) KLC1-ALK: A Novel Fusion in Lung Cancer Identified Using a Formalin-Fixed Paraffin-Embedded Tissue Only. PLoS ONE 7(2): e31323. doi:10.1371/journal.pone.0031323

Editor: Anthony W.I. Lo, The Chinese University of Hong Kong, Hong Kong

Received October 17, 2011; **Accepted** January 5, 2012; **Published** February 8, 2012

Funding: This work was supported in part by Grants-in-Aid for Scientific Research from the Ministry of Education, Culture, Sports, Science, and Technology of Japan as well as by grants from the Japan Society for the Promotion of Science; the Ministry of Health, Labor, and Welfare of Japan; the Vehicle Racing Commemorative Foundation of Japan; the Princess Takamatsu Cancer Research Fund; and the Uehara Memorial Foundation. The funders had no role in study design, data collection and analysis, decision to publish, or preparation of the manuscript.

Competing Interests: The authors have declared that no competing interests exist.

* E-mail: kentakeuchi-tky@umin.net

Introduction

Anaplastic lymphoma kinase (ALK) is a receptor tyrosine kinase that was discovered in anaplastic large-cell lymphoma (ALCL) in the form of a fusion protein, NPM-ALK [1,2]. The formation of a fusion protein with a partner through chromosomal translocations is the most common mechanism of ALK overexpression and ALK kinase domain activation. Recent promising results of clinical trials with an ALK inhibitor, crizotinib, have changed the significance of ALK fusions in lung cancer [3,4,5,6], inflammatory myofibroblastic tumors (IMTs) [7], and ALCL [8]. ALK fusions are no longer mere research targets or diagnostic markers and are now directly linked to the therapeutic benefit of patients.

In lung cancer, 3 fusion partners of ALK have been reported—EML4, TFG, and KIF5B—although the presence of TFG-ALK in lung cancer has not yet been proven with histopathological evidence [9,10,11]. In addition to lung cancer, ALK has further been found to generate fusions in ALCL (fused to NPM, TPM3, TPM4, ATIC, TFG, CLTC, MSN, MYH9, or ALO17) [1,2,12,13,14,15,16,17,18,19], IMT (TPM3, TPM4, CLTC, CARS, RANBP2, ATIC, or SEC31A) [19,20,21,22,23,24], ALK-positive large B-cell lymphoma (CLTC, NPM, SEC31A, or SQSTM1) [25,26,27,28], and renal cancer (VCL, TPM3 or EML4) (Table 1) [29,30]. In addition to TFG-ALK in lung cancer, some ALK fusions have been reported without histopathological evidence: TPM4-ALK in esophageal squamous cell carcinoma [31,32] and EML4-ALK in colon and breast carcinomas [33].

Anti-ALK immunohistochemistry played an important role in identifying these ALK fusion partners. Several ALK fusions exhibit a characteristic staining pattern in anti-ALK immunohistochemistry because the subcellular localization of ALK fusion proteins depends on the fusion partner. For example, NPM-ALK, which is the most common fusion in ALK-positive ALCL (85%), exhibits a nuclear and cytoplasmic staining pattern because the heterodimer of NPM and NPM-ALK localizes in the nucleus and the homodimer of NPM-ALK in the cytoplasm; CLTC-ALK exhibits a cytoplasmic granular pattern because it localizes in the small vesicles. If a tumor exhibits an unrecognized anti-ALK staining pattern, the patient may have a novel fusion partner. In addition to the difference in subcellular localization, the difference in staining intensity is a key to identifying novel partners. EML4-ALK is hardly stained by conventional anti-ALK immunohistochemistry [11,34]. To overcome this limitation, we developed the intercalated antibody-enhanced polymer (iAEP) method, which moderately increases

Table 1. ALK fusion partners.

Reported year	Partner	Locus	ALK+ALCL	ALK+LBCL	IMT	NSCLC	RCC
1994	NPM	5q35.1	+	+			
1999	TPM3	1p23	+		+		+
1999	TFG	3q12.2	+			+*	
2000	ATIC	2q35	+		+		
2000	TPM4	19p13	+		+		
2001	CLTC	17q23	+	+	+		
2001	MSN	Xp11.1	+				
2002	ALO17	17q25.3	+				
2003	MYH9	22q13.1	+				
2003	RANBP2	2q13			+		
2003	CARS	11p15			+		
2006	SEC31A	4q41		+	+		
2007	EML4	2p21				+	+
2009	KIF5B	10p11.22				+	
2011	SQSTM1	5q35.3		+			
2011	PPFIBP1	12p11			+		
2011	VCL	10q22.2					+
Present study	KLC1	14q32.1				+	

*Histopathological evidence is lacking. Abbreviations: ALCL, anaplastic large cell lymphoma; LBCL, large B-cell lymphoma; IMT, inflammatory myofibroblastic tumor; NSCLC, non-small cell lung carcinoma; RCC, renal cell carcinoma.
doi:10.1371/journal.pone.0031323.t001

sensitivity in the immunohistochemical detection system, and EML4-ALK was consistently stained with this method [11]. This indicated that a tumor that is positively immunostained for ALK only by a sensitive immunohistochemistry method but not by conventional methods may harbor a novel ALK fusion. Based on this hypothesis, we successfully identified PPFIBP1-ALK in 2 IMT cases that were positive in anti-ALK immunohistochemistry only when stained by the iAEP method [35].

Anti-ALK immunohistochemistry may thus be useful to detect candidate tumors for a novel ALK fusion. However, to identify the fusion partner, other molecular techniques are usually required such as 5′-rapid amplification of cDNA ends (5′-RACE) or inverse reverse-transcription polymerase chain reaction (RT-PCR). To the best of our knowledge, no novel oncogenic fusions have been discovered using formalin-fixed paraffin-embedded (FFPE) tissues only because nucleic acids extracted from FFPE tissues are severely degraded during the fixation process. In the present study, we developed a 5′-RACE method optimized for *ALK* fusion partner detection that was applicable to FFPE tissues and identified a novel fusion, kinesin light chain 1 (KLC1)-ALK, in lung cancer by using only an FFPE tissue.

Methods

Materials

A FFPE tissue block of pulmonary adenocarcinoma in situ, nonmucinous (formerly called bronchioloalveolar carcinoma) [36], which was excised from a 47-year-old female patient was used [37]. This carcinoma was negative for EML4-ALK and KIF5B-ALK, although the presence of *ALK* rearrangement was confirmed by anti-ALK iAEP immunohistochemistry and a split fluorescence in situ hybridization (FISH) assay for ALK (hereafter referred to as the unknown ALK fusion-positive case) (Figure 1) [37]. Two FFPE tissue blocks of ALK-positive tumor cases were also employed, for which the presence of EML4-ALK or KIF5B-ALK had already been confirmed. Total RNA was extracted from each FFPE tissue with the use of the RecoverAll™ Total Nucleic Acid Isolation Kit for FFPE (Applied Biosystems Japan, Tokyo, Japan). The ages of the 3 FFPE blocks used (time from FFPE tissue production to RNA extraction) were 65, 40, and 51 months for the unknown ALK fusion-positive case, EML4-ALK, and KIF5B-ALK, respectively. Written informed consent was obtained from each patient. The study was approved by the institutional review board of the Shizuoka Cancer Center (approval ID 22-J132-22-1) and the Japanese Foundation for Cancer Research (approval ID 2010-1011).

Modified 5′-RACE for ALK fusions applicable to FFPE tissues

5′-RACE was performed with the SMARTer RACE cDNA Amplification Kit (Clontech) according to the manufacturer's instruction with minor modifications. In brief, instead of the primers included in the kit, ALK-3242R (5′-CTCAGCTTG-TACTCAGGGC-3′) was used for cDNA synthesis. The cDNA was subjected to 5′-RACE PCR using PrimeSTAR HS DNA Polymerase (TaKaRa) and the following primers: Universal Primer A Mix of the kit and ALK-3206R (5′-ATGGCTTG-CAGCTCCTGGTGCTT-3′). The PCR condition consisted of 5 cycles at 94°C for 30 s and 72°C for 3 min; 5 cycles at 94°C for 30 s, 70°C for 30 s, and 72°C for 3 min; and 30 cycles at 94°C for 30 s, 68°C for 30 s, and 72°C for 3 min.

FISH

FISH analysis of fusion genes was performed with DNA probes for KLC1 and ALK. Unstained sections (4-μm thick) were subjected to hybridization with an ALK-split probe set (Dako, Tokyo, Japan) or with bacterial artificial chromosome (BAC) clone-derived probes for ALK (RP11-984I21 and RP11-62B19)

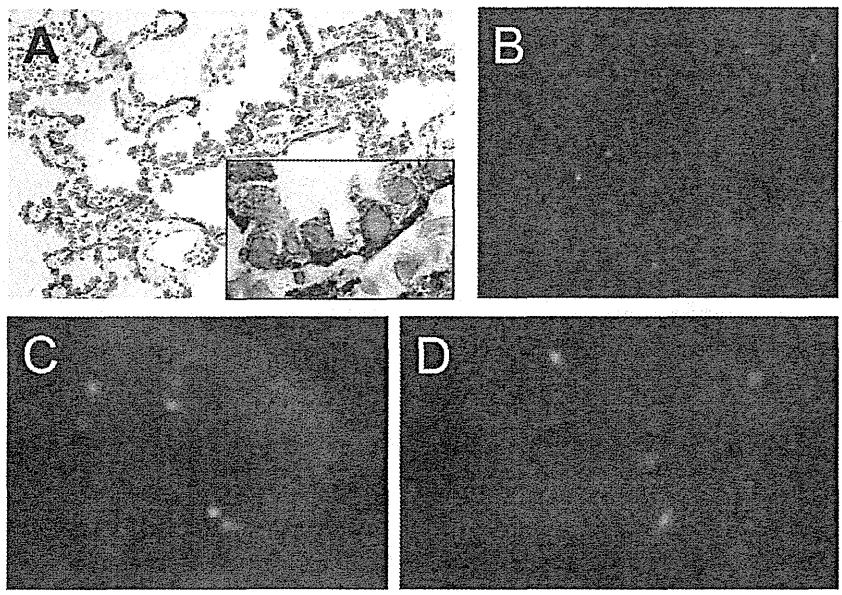

Figure 1. ALK-rearranged lung adenocarcinoma without EML4-ALK and KIF5B-ALK. Panel A shows the results of anti-ALK immunohistochemistry with the iAEP method on pulmonary adenocarcinoma in situ, nonmucinous. The staining pattern was diffusely cytoplasmic. The basal side of tumor cells was more strongly stained, indicating an uneven subcellular localization of KLC1-ALK protein. FISH analyses revealed that this case was positive in the split assay for *ALK* (Panel B: individual 5′- and 3′-signals are observed) and negative in *EML4-ALK* and *KIF5B-ALK* fusion assays (Panel C: *EML4*, red; *ALK*, green; Panel D: *KIF5B*, green; *ALK*, red).
doi:10.1371/journal.pone.0031323.g001

and KLC1 (RP11-186F6). Hybridized slides were then stained with DAPI and examined using a BX51 fluorescence microscope (Olympus, Tokyo, Japan).

Synthesis of the putative cDNA of *KLC1-ALK*

Two independent PCRs were performed using cDNA synthesized from a tumor tissue expressing KIF5B-ALK with the following primer sets: KLC1-NheI-M (5′-GCGCTAGCGAATGTATGACAACATGTCCAC-3′) and KLC1-bpR (5′-GTGCTTCCGGCGGTACACATCTACAGAACCAAACTC-3′), and ALK-bpF (5′-GGGAGTTTGGTTCTGTAGATGTGTACCGCCGGAAGC-3′) and ALK-EcoRI (5′-GATAGAATTCTCAGGGCCCAGGCT-3′). Then, the second PCR was performed using a 1/100 dilution of a mixture of the first PCR products as a template with the KLC1-NheI-M and ALK-EcoRI primers (Figure 2).

Transformation assay for *KLC1-ALK*

Analysis of the transforming activity of kinase fusions was performed as described previously [9,38,39]. A pMXS-based expression plasmid for each fusion was used to generate recombinant ecotropic retroviruses [40], which were then used individually to infect mouse 3T3 fibroblasts. The formation of transformed foci was evaluated after culturing the cells for 4 days. The same set of 3T3 cells was injected subcutaneously into nu/nu mice, and tumor formation was examined after 14 days. The animal experiments were approved by the animal ethics committee of Jichi Medical University (approval ID 1135).

Results

Identification of *KLC1-ALK* as a novel *ALK* fusion gene

Our modified 5′-RACE faithfully isolated cDNA fragments for *EML4-ALK* or *KIF5B-ALK* from known ALK- positive tumors (Supplementary Figure S1A and B). We then attempted to isolate cDNA fragments encompassing the fusion points from the unknown ALK fusion-positive case. Nucleotide sequencing of such 5′-RACE products revealed that 2 of 10 clones contained the 3′-terminus of exon 9 of *KLC1* (ENST00000348520) fused to the first nucleotide of exon 20 of *ALK* (ENST00000389048), indicating the presence of a novel fusion between *KLC1* and *ALK*. As this rearrangement constituted an in-frame fusion between the 2 genes, the full-length *KLC1-ALK* cDNA probably produces a protein of 984 amino acids containing an amino-terminal two-thirds of KLC1 and an intracellular region of ALK (Figure 3A). RT-PCR-mediated isolation of a fusion point successfully confirmed the in-frame fusion between the 2 messages (Figure 3A and B). Further, to confirm the genomic rearrangement responsible for the fusion, a fusion FISH assay was performed (Figure 3C). These results were consistent with the presence of t(2;14)(p23;q32.3), leading to the generation of *KLC1-ALK*.

Transforming potential of *KLC1-ALK*

The putative full-length cDNA of *KLC1-ALK* was synthesized from the frozen tissue with KIF5B-ALK fusion expression (Figure 2, Supplementary Figure S2), and was used to generate a recombinant retrovirus expressing the fusion protein with an amino-terminal FLAG epitope tag. Infection of 3T3 cells with the virus expressing KLC1-ALK readily produced multiple transformed foci in culture and subcutaneous tumors in a nude mouse tumorigenicity assay (Figure 4), confirming the potent transforming ability of KLC1-ALK.

Discussion

Here, by analyzing the FFPE tissues only, we successfully discovered a novel ALK fusion, KLC1-ALK. While snap-frozen materials sampled from biopsied or surgically removed specimens

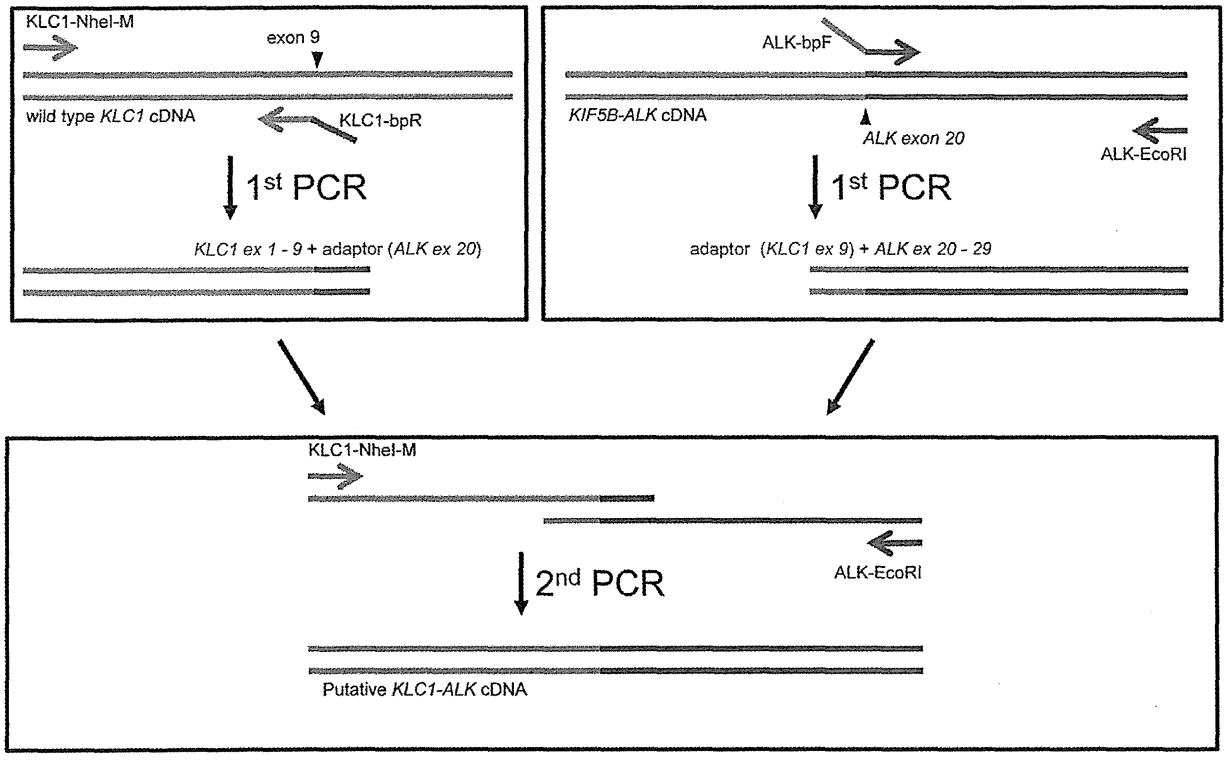

Figure 2. Synthesis of the putative KLC1-ALK full-length cDNA. Two first-round PCRs were performed separately using cDNA synthesized from a tumor tissue expressing KIF5B-ALK with the following primer sets: KLC1-NheI-M and KLC1-bpR, and ALK-bpF and ALK-EcoRI. KLC1-bpR and ALK-bpF had sequences downstream of the ALK break point (exon 20) and upstream of the KLC1 break point (exon 9) as adopter sequences, respectively. Then, the second PCR was performed using a 1/100 dilution of the mixture of the first PCR products as a template with primers KLC1-NheI-M and ALK-EcoRI. The first PCR products were annealed, extended with each other, and then amplified with the primers.
doi:10.1371/journal.pone.0031323.g002

can be used for various types of molecular analyses, they are not routinely sampled in most clinical settings. In contrast, FFPE specimens are usually produced, and histopathology diagnostic archives are an extremely large resource of FFPE tissues in ordinary diagnostic pathology laboratories. However, DNA and RNA extracted from FFPE tissues are severely degraded during formalin fixation and are usually not suitable for assays that need long DNA/RNA of high quality. Recent technical advances have allowed some analyses for known point mutations and known fusion genes, but it is still difficult to identify an unrecognized gene aberration using only an FFPE tissue.

In most *ALK* fusions, the break point of *ALK* is located within intron 19, and the fusion point in mRNA is typically the first nucleotide of exon 20. Therefore, if the primers for 5′-RACE are placed immediately downstream of the first nucleotide of *ALK* exon 20, such 5′-RACE may successfully isolate PCR products containing the partner gene sequence even using FFPE tissues. Based on this hypothesis, we established a 5′-RACE system for *ALK* fusions optimized for FFPE tissues. With this system, we identified a novel *ALK* fusion, *KLC1-ALK*. To the best of our knowledge, this is the first novel oncogenic fusion identified using only an FFPE tissue.

Caution, however, is needed. In some rare cases with *ALK* fusion, the break point of *ALK* fusion mRNA may not be at the 5′-end of exon 20. For example, in variant 4 of *EML4-ALK*, exon 14 of *EML4* is fused to an unknown sequence of 11 bp, which in turn is connected to nucleotide 50 of *ALK* exon 20 (E14;ins11;del49A20) [38]. Our 5′-RACE system would not work on such a case because the reverse primer ALK-3206R corresponds to nucleotides 12–34 of *ALK* exon 20. Therefore, if our modified 5′-RACE fails to isolate fusion cDNAs from cases with a confirmed ALK rearrangement, other primer settings may be attempted.

Kinesin is a heterotetramer of 2 kinesin heavy chains and 2 kinesin light chains, and it moves on the microtubules towards their plus ends carrying various cargos. The heavy chains harbor the motor activity, whereas the light chains play roles in cargo binding and in modulating the activity and subcellular localization of the heavy chains. KLC1 binds to the kinesin heavy chains with an N-terminal domain and to various cargos via the tetratricopeptide repeat domains [41,42]. Of the 3 histopathologically confirmed ALK fusion partners in lung cancer, EML4 colocalizes with microtubules and may contribute to the stabilization of microtubules [43], KIF5B moves on the microtubules as a kinesin heavy chain [44], and KLC1 binds to kinesin heavy chains as a kinesin light chain. Therefore, it is interesting that all the 3 ALK fusions in lung cancer are likely to colocalize with microtubules.

The most frequent ALK fusion in lung cancer is EML4-ALK (4–7%) [9,38], and the second is KIF5B-ALK (0.5%) [11]. One case with TFG-ALK is reported [10]. KLC1-ALK may be rare but exists in lung adenocarcinoma, and the patients with this fusion are highly likely to benefit from ALK inhibitor therapy as do patients with other ALK fusions. The incidence may be low, but the significance of this fusion is very high from the perspective

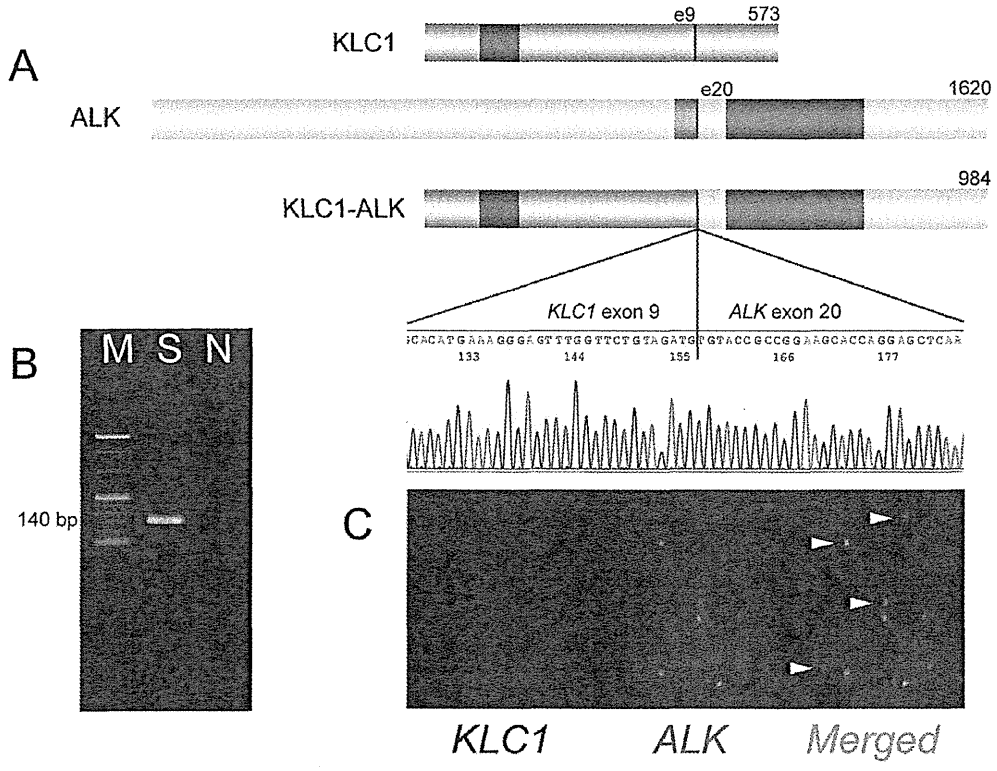

Figure 3. Identification of KLC1-ALK. Panel A shows the schematic structure of KLC1, ALK, and KLC1-ALK proteins and the cDNA sequence around the fusion point. Dark blue, orange, and red parts represent coiled-coil, transmembrane, and kinase domains, respectively. The break point exons and the number of amino acids are indicated. KLC1-ALK-specific RT-PCR using RNA extracted from the FFPE tissue of the unknown ALK fusion-positive case amplified a fragment of the expected product size (140 bp, Panel B) with the consistent fusion sequence (Panel A). A fusion FISH assay for *KLC1-ALK* revealed a fusion signal (yellow) in multiple tumor cells (Panel C). M, marker (100-bp ladder); S, sample (the unknown ALK fusion-positive case); N, no template control.
doi:10.1371/journal.pone.0031323.g003

of a tailor-made therapeutic option for the patient. Another important point is that KLC1-ALK was found in adenocarcinoma in situ, nonmucinous (formerly called bronchioloalveolar carcinoma, BAC). BAC is recognized to rarely harbor ALK fusions, although a small number of BAC cases has been examined for ALK fusion compared with invasive adenocarcinoma. It would be interesting from a pathobiological perspective to examine a large-scale cohort of BAC and other premalignant conditions for ALK fusion.

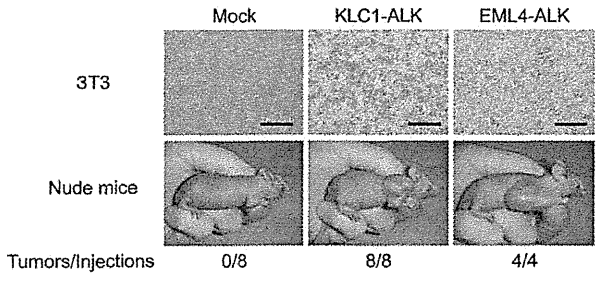

Figure 4. Transforming potential of KLC1-ALK. Upper panels: Mouse 3T3 fibroblasts were infected with retroviruses encoding KLC1-ALK or EML4-ALK or with the corresponding empty virus (Mock). The cells were photographed after 4 days of culture. Scale bar, 1 mm. Lower panels: Nude mice were injected subcutaneously with the corresponding 3T3 cells, and tumor formation was examined after 14 days. The number of tumors formed per injections is indicated at the bottom.
doi:10.1371/journal.pone.0031323.g004

There are 3 methods for the detection of ALK fusions: RT-PCR, ALK split FISH, and high-sensitivity anti-ALK immunohistochemistry. For RT-PCR, the 5′ partner gene must be known. Our findings in this study identified one more partner gene that should be targeted in ALK-fusion detection using RT-PCR in lung cancer. The other 2 methods can detect all ALK fusions regardless of fusion partner and, therefore, are suitable for ALK-fusion screening. In other words, these 2 methods cannot identify the fusion partner and need to be succeeded by partner-specific RT-PCR and/or fusion FISH for this purpose. If it is revealed that the partner gene in the tested case is unknown, a novel partner gene is highly likely to be discovered, as was shown in the present study. In fact, using high-sensitivity anti-ALK immunohistochemistry (iAEP method) as screening, we have identified several novel ALK fusions in various types of cancers including lung adenocarcinoma [11], lymphoma [28], sarcoma [35], and renal cell carcinoma [30].

Many efficient tools have been established for the detection of ALK fusion-positive cases using FFPE tissues, including anti-ALK immunohistochemistry and FISH. Our findings will further expand the potential value of archival FFPE tissues and provide further biological and clinical insights into ALK-positive cancers in the forthcoming era of ALK inhibitor therapy.

Supporting Information

Figure S1 5′-RACE products using FFPE tissues. Our modified 5′-RACE faithfully isolated cDNA fragments for *EML4-ALK* (A) or *KIF5B-ALK* (B) from known ALK- positive tumors.
(TIF)

Figure S2 Putative cDNA sequence of KLC1-ALK. The putative full-length cDNA of *KLC1-ALK* was synthesized from the frozen tissue with KIF5B-ALK fusion expression.
(PDF)

Acknowledgments

We thank Mr. Motoyoshi Iwakoshi, Ms. Keiko Shiozawa, Ms. Tomoyo Kakita, and Ms. Kimie Nomura for their technical assistance, and Ms. Sayuri Sengoku for providing administrative assistance.

Author Contributions

Conceived and designed the experiments: KT HM. Performed the experiments: YT MS SS ES SH RA. Analyzed the data: YT MS HM KT. Contributed reagents/materials/analysis tools: RA TN. Wrote the paper: KT HM.

References

1. Morris SW, Kirstein MN, Valentine MB, Dittmer KG, Shapiro DN, et al. (1994) Fusion of a kinase gene, ALK, to a nucleolar protein gene, NPM, in non-Hodgkin's lymphoma. Science 263: 1281–1284.
2. Shiota M, Fujimoto J, Semba T, Satoh H, Yamamoto T, et al. (1994) Hyperphosphorylation of a novel 80 kDa protein-tyrosine kinase similar to Ltk in a human Ki-1 lymphoma cell line, AMS3. Oncogene 9: 1567–1574.
3. Kwak EL, Bang YJ, Camidge DR, Shaw AT, Solomon B, et al. (2010) Anaplastic lymphoma kinase inhibition in non-small-cell lung cancer. N Engl J Med 363: 1693–1703.
4. Kimura H, Nakajima T, Takeuchi K, Soda M, Mano H, et al. (2011) ALK fusion gene positive lung cancer and 3 cases treated with an inhibitor for ALK kinase activity. Lung Cancer.
5. Kijima T, Takeuchi K, Tetsumoto S, Shimada K, Takahashi R, et al. (2011) Favorable response to crizotinib in three patients with echinoderm microtubule-associated protein-like 4-anaplastic lymphoma kinase fusion-type oncogene-positive non-small cell lung cancer. Cancer Sci 102: 1602–1604.
6. Nakajima T, Kimura H, Takeuchi K, Soda M, Mano H, et al. (2010) Treatment of Lung Cancer with an ALK Inhibitor After EML4-ALK Fusion Gene Detection Using Endobronchial Ultrasound-Guided Transbronchial Needle Aspiration. J Thorac Oncol 5: 2041–2043.
7. Butrynski JE, D'Adamo DR, Hornick JL, Dal Cin P, Antonescu CR, et al. (2010) Crizotinib in ALK-rearranged inflammatory myofibroblastic tumor. N Engl J Med 363: 1727–1733.
8. Gambacorti-Passerini C, Messa C, Pogliani EM (2011) Crizotinib in anaplastic large-cell lymphoma. N Engl J Med 364: 775–776.
9. Soda M, Choi YL, Enomoto M, Takada S, Yamashita Y, et al. (2007) Identification of the transforming EML4-ALK fusion gene in non-small-cell lung cancer. Nature 448: 561–566.
10. Rikova K, Guo A, Zeng Q, Possemato A, Yu J, et al. (2007) Global survey of phosphotyrosine signaling identifies oncogenic kinases in lung cancer. Cell 131: 1190–1203.
11. Takeuchi K, Choi YL, Togashi Y, Soda M, Hatano S, et al. (2009) KIF5B-ALK, a novel fusion oncokinase identified by an immunohistochemistry-based diagnostic system for ALK-positive lung cancer. Clin Cancer Res 15: 3143–3149.
12. Lamant L, Dastugue N, Pulford K, Delsol G, Mariame B (1999) A new fusion gene TPM3-ALK in anaplastic large cell lymphoma created by a (1;2)(q25;p23) translocation. Blood 93: 3088–3095.
13. Meech SJ, McGavran L, Odom LF, Liang X, Meltesen L, et al. (2001) Unusual childhood extramedullary hematologic malignancy with natural killer cell properties that contains tropomyosin 4–anaplastic lymphoma kinase gene fusion. Blood 98: 1209–1216.
14. Colleoni GW, Bridge JA, Garicochea B, Liu J, Filippa DA, et al. (2000) ATIC-ALK: A novel variant ALK gene fusion in anaplastic large cell lymphoma resulting from the recurrent cryptic chromosomal inversion, inv(2)(p23q35). Am J Pathol 156: 781–789.
15. Hernandez L, Pinyol M, Hernandez S, Bea S, Pulford K, et al. (1999) TRK-fused gene (TFG) is a new partner of ALK in anaplastic large cell lymphoma producing two structurally different TFG-ALK translocations. Blood 94: 3265–3268.
16. Touriol C, Greenland C, Lamant L, Pulford K, Bernard F, et al. (2000) Further demonstration of the diversity of chromosomal changes involving 2p23 in ALK-positive lymphoma: 2 cases expressing ALK kinase fused to CLTCL (clathrin chain polypeptide-like). Blood 95: 3204–3207.
17. Tort F, Pinyol M, Pulford K, Roncador G, Hernandez L, et al. (2001) Molecular characterization of a new ALK translocation involving moesin (MSN-ALK) in anaplastic large cell lymphoma. Lab Invest 81: 419–426.
18. Lamant L, Gascoyne RD, Duplantier MM, Armstrong F, Raghab A, et al. (2003) Non-muscle myosin heavy chain (MYH9): a new partner fused to ALK in anaplastic large cell lymphoma. Genes Chromosomes Cancer 37: 427–432.
19. Cools J, Wlodarska I, Somers R, Mentens N, Pedeutour F, et al. (2002) Identification of novel fusion partners of ALK, the anaplastic lymphoma kinase, in anaplastic large-cell lymphoma and inflammatory myofibroblastic tumor. Genes Chromosomes Cancer 34: 354–362.
20. Lawrence B, Perez-Atayde A, Hibbard MK, Rubin BP, Dal Cin P, et al. (2000) TPM3-ALK and TPM4-ALK oncogenes in inflammatory myofibroblastic tumors. Am J Pathol 157: 377–384.
21. Bridge JA, Kanamori M, Ma Z, Pickering D, Hill DA, et al. (2001) Fusion of the ALK gene to the clathrin heavy chain gene, CLTC, in inflammatory myofibroblastic tumor. Am J Pathol 159: 411–415.
22. Ma Z, Hill DA, Collins MH, Morris SW, Sumegi J, et al. (2003) Fusion of ALK to the Ran-binding protein 2 (RANBP2) gene in inflammatory myofibroblastic tumor. Genes Chromosomes Cancer 37: 98–105.
23. Debiec-Rychter M, Marynen P, Hagemeijer A, Pauwels P (2003) ALK-ATIC fusion in urinary bladder inflammatory myofibroblastic tumor. Genes Chromosomes Cancer 38: 187–190.
24. Panagopoulos I, Nilsson T, Domanski HA, Isaksson M, Lindblom P, et al. (2006) Fusion of the SEC31L1 and ALK genes in an inflammatory myofibroblastic tumor. Int J Cancer 118: 1181–1186.
25. Delsol G, Lamant L, Mariame B, Pulford K, Dastugue N, et al. (1997) A new subtype of large B-cell lymphoma expressing the ALK kinase and lacking the 2; 5 translocation. Blood 89: 1483–1490.
26. Gascoyne RD, Lamant L, Martin-Subero JI, Lestou VS, Harris NL, et al. (2003) ALK-positive diffuse large B-cell lymphoma is associated with Clathrin-ALK rearrangements: report of 6 cases. Blood 102: 2568–2573.
27. Van Roosbroeck K, Cools J, Dierickx D, Thomas J, Vandenberghe P, et al. (2010) ALK-positive large B-cell lymphomas with cryptic SEC31A-ALK and NPM1-ALK fusions. Haematologica 95: 509–513.
28. Takeuchi K, Soda M, Togashi Y, Ota Y, Sekiguchi Y, et al. (2010) Identification of a novel fusion, SQSTM1-ALK, in ALK-positive large B-cell lymphoma. Haematologica.
29. Debelenko LV, Raimondi SC, Daw N, Shivakumar BR, Huang D, et al. (2011) Renal cell carcinoma with novel VCL-ALK fusion: new representative of ALK-associated tumor spectrum. Mod Pathol 24: 430–442.
30. Sugawara E, Togashi Y, Kuroda N, Sakata S, Hatano S, et al. (in press) Identification of ALK Fusions in Renal Cancer: Large-Scale Immunohistochemical Screening by intercalated Antibody-Enhanced Polymer Method. Cancer.
31. Du XL, Hu H, Lin DC, Xia SH, Shen XM, et al. (2007) Proteomic profiling of proteins dysregulted in Chinese esophageal squamous cell carcinoma. J Mol Med 85: 863–875.
32. Jazii FR, Najafi Z, Malekzadeh R, Conrads TP, Ziaee AA, et al. (2006) Identification of squamous cell carcinoma associated proteins by proteomics and loss of beta tropomyosin expression in esophageal cancer. World J Gastroenterol 12: 7104–7112.
33. Lin E, Li L, Guan Y, Soriano R, Rivers CS, et al. (2009) Exon array profiling detects EML4-ALK fusion in breast, colorectal, and non-small cell lung cancers. Mol Cancer Res 7: 1466–1476.
34. Martelli MP, Sozzi G, Hernandez L, Pettirossi V, Navarro A, et al. (2009) EML4-ALK rearrangement in non-small cell lung cancer and non-tumor lung tissues. Am J Pathol 174: 661–670.
35. Takeuchi K, Soda M, Togashi Y, Sugawara E, Hatano S, et al. (2011) Pulmonary inflammatory myofibroblastic tumor expressing a novel fusion, PPFIBP1-ALK: reappraisal of anti-ALK immunohistochemistry as a tool for novel ALK fusion identification. Clin Cancer Res 17: 3341–3348.
36. Travis WD, Brambilla E, Noguchi M, Nicholson AG, Geisinger KR, et al. (2011) International association for the study of lung cancer/american thoracic society/european respiratory society international multidisciplinary classification of lung adenocarcinoma. J Thorac Oncol 6: 244–285.
37. Yamamoto M, Takeuchi K, Shimoji M, Maniwa T, Isaka M, et al. (in press) Small non-mucinous bronchioloalveolar carcinoma with ALK immunoreactivity: A novel ALK fusion gene? Cancer Sci.
38. Takeuchi K, Choi YL, Soda M, Inamura K, Togashi Y, et al. (2008) Multiplex reverse transcription-PCR screening for EML4-ALK fusion transcripts. Clin Cancer Res 14: 6618–6624.
39. Choi YL, Takeuchi K, Soda M, Inamura K, Togashi Y, et al. (2008) Identification of novel isoforms of the EML4-ALK transforming gene in non-small cell lung cancer. Cancer Res 68: 4971–4976.
40. Onishi M, Kinoshita S, Morikawa Y, Shibuya A, Phillips J, et al. (1996) Applications of retrovirus-mediated expression cloning. Exp Hematol 24: 324–329.
41. Stenoien DL, Brady ST (1997) Immunochemical analysis of kinesin light chain function. Mol Biol Cell 8: 675–689.

42. Rahman A, Kamal A, Roberts EA, Goldstein LS (1999) Defective kinesin heavy chain behavior in mouse kinesin light chain mutants. J Cell Biol 146: 1277–1288.
43. Houtman SH, Rutteman M, De Zeeuw CI, French PJ (2007) Echinoderm microtubule-associated protein like protein 4, a member of the echinoderm microtubule-associated protein family, stabilizes microtubules. Neuroscience 144: 1373–1382.
44. Sablin EP (2000) Kinesins and microtubules: their structures and motor mechanisms. Curr Opin Cell Biol 12: 35–41.

nature medicine

RET, ROS1 and ALK fusions in lung cancer

Kengo Takeuchi[1,2], Manabu Soda[3], Yuki Togashi[1,2], Ritsuro Suzuki[4], Seiji Sakata[1], Satoko Hatano[1], Reimi Asaka[1,2], Wakako Hamanaka[2], Hironori Ninomiya[2], Hirofumi Uehara[5], Young Lim Choi[6], Yukitoshi Satoh[5,7], Sakae Okumura[5], Ken Nakagawa[5], Hiroyuki Mano[3,6] & Yuichi Ishikawa[2]

Through an integrated molecular- and histopathology-based screening system, we performed a screening for fusions of anaplastic lymphoma kinase (ALK) and c-ros oncogene 1, receptor tyrosine kinase (ROS1) in 1,529 lung cancers and identified 44 ALK-fusion–positive and 13 ROS1-fusion–positive adenocarcinomas, including for unidentified fusion partners for ROS1. In addition, we discovered previously unidentified kinase fusions that may be promising for molecular-targeted therapy, kinesin family member 5B (KIF5B)-ret proto-oncogene (RET) and coiled-coil domain containing 6 (CCDC6)-RET, in 14 adenocarcinomas. A multivariate analysis of 1,116 adenocarcinomas containing these 71 kinase-fusion–positive adenocarcinomas identified four independent factors that are indicators of poor prognosis: age ≥50 years, male sex, high pathological stage and negative kinase-fusion status.

Echinoderm microtubule associated protein like 4 (EML4)-ALK was the first targetable fusion oncokinase to be identified in non–small cell lung cancer (NSCLC)[1]. This fusion is found in approximately 4–6% of lung adenocarcinomas[2,3]. ROS1 is another receptor tyrosine kinase that forms fusions in NSCLC[4]. Solute carrier family 34 (sodium phosphate), member 2 (SLC34A2)-ROS1 and CD74 molecule, major histocompatibility complex, class II invariant chain (CD74)-ROS1 were identified in 1 out of 41 NSCLC cell lines and 1 out of 150 lung cancer samples, respectively[4]. However, the oncogenic ability of these ROS1 fusion proteins and the incidence of ROS1 fusions in lung cancers are still unclear.

We screened for known and unknown kinase fusions in lung cancers using a histopathology-based system with tissue microarrays of 1,528 surgically removed tissues (**Supplementary Methods** and **Supplementary Appendix**). Immunohistochemistry of antibodies to ALK using the intercalated antibody-enhanced polymer method[2,3,5–7] detected 45 tumors with ALK kinase domain expression (**Supplementary Fig. 1**). In 44 adenocarcinomas, multiplex RT-PCR[2,3] identified 41 *EML4-ALK*–positive and 3 *KIF5B-ALK*–positive adenocarcinomas, including a previously unidentified KIF5B-ALK fusion variant, K17;A20 (**Supplementary Table 1**). Further, we used fluorescence *in situ* hybridization (FISH) for split and fusion assays to confirm the presence of ALK fusions[2,3,8]. The FISH results for the *ALK* split assay, the *EML4-ALK* fusion assay and the *KIF5B-ALK* fusion assay in the 44 adenocarcinomas were all consistent with the presence of the corresponding fusion gene (**Supplementary Figs. 2** and **3**). The remaining tumor that was positive for antibodies to ALK as determined by immunohistochemistry (a large-cell neuroendocrine carcinoma) was negative in the FISH assays and expressed wild-type ALK. ALK fusions existed in 3.0% (44 out of 1,485) of the NSCLCs and 3.9% (44 out of 1,121) of the adenocarcinomas. We included 20 previously reported ALK-fusion–positive and 304 ALK-fusion–negative tumors, all of which were screened with multiplex RT-PCR. Because specimens of these 324 patients were collected consecutively during the period of tissue collection, they served as positive and negative controls, respectively[1–3,8,9]. The immunohistochemistry results using the intercalated antibody-enhanced polymer method were complete matches in the 20 fusion-positive and the 304 fusion-negative tumors.

We used split FISH assays for the screening for *ROS1* gene rearrangement (**Fig. 1**). In 11 of the 13 *ROS1* split FISH-positive tumors (**Fig. 1a**), 5′ rapid amplification of complementary DNA ends (5′ RACE) identified two known and three unknown fusion partners for *ROS1*: *TPM3*, *SDC4*, *SLC34A2*, *CD74* and *EZR* (**Fig. 1b** and **Supplementary Table 1**); RT-PCR confirmed this finding (**Fig. 1c**). In a 5′-RACE–negative tumor (ROS#12) (again, where split FISH is used to detect candidate fusion genes of interest by the presence of rearrangements and RACE is used for the identification of fusion partners), each fusion-specific RT-PCR (using a common reverse primer) amplified the same band, which contained an *LRIG3* sequence. This tumor was proven fusion-positive in RT-PCR specific to *LRIG3-ROS1*, an unidentified fusion. Fusion FISH results confirmed that all 12 cases harbored the corresponding fusion (**Fig. 1a**). All fusion FISH assays for these six ROS1 fusions were negative for the tumor ROS#13 (the frozen material had been consumed), indicating an unknown fusion partner for *ROS1*. *ROS1* split FISH screening failed for nine NSCLCs, including five adenocarcinomas. We identified ROS1 fusions in 0.9% (13 out of 1,476) of the NSCLCs and 1.2% (13 out of 1,116) of the adenocarcinomas.

We performed *KIF5B* split FISH to discover new fusion kinases, as we previously identified KIF5B-ALK fusions in lung cancer[3]. As such, we hypothesized that KIF5B might be rearranged in lung cancer. In 24 *KIF5B* split FISH-positive tumors, 3′ RACE identified an in-frame fusion between *KIF5B* exon 23 and *RET* exon 12

[1]Pathology Project for Molecular Targets, the Cancer Institute, Japanese Foundation for Cancer Research, Tokyo, Japan. [2]Division of Pathology, the Cancer Institute, Japanese Foundation for Cancer Research, Tokyo, Japan. [3]Division of Functional Genomics, Jichi Medical University, Tochigi, Japan. [4]Department of Hematopoietic Stem Cell Transplantation Data Management and Biostatistics, Nagoya University Graduate School of Medicine, Nagoya, Japan. [5]Department of Thoracic Surgical Oncology, Thoracic Center, the Cancer Institute Hospital, Japanese Foundation for Cancer Research, Tokyo, Japan. [6]Department of Medical Genomics, Graduate School of Medicine, University of Tokyo, Tokyo, Japan. [7]Present address: Department of Thoracic Surgery, Kitasato University School of Medicine, Kanagawa, Japan. Correspondence should be addressed to K.T. (kentakeuchi-tky@umin.net).

Received 28 September 2011; accepted 3 January 2012; published online 12 February 2012; doi:10.1038/nm.2658

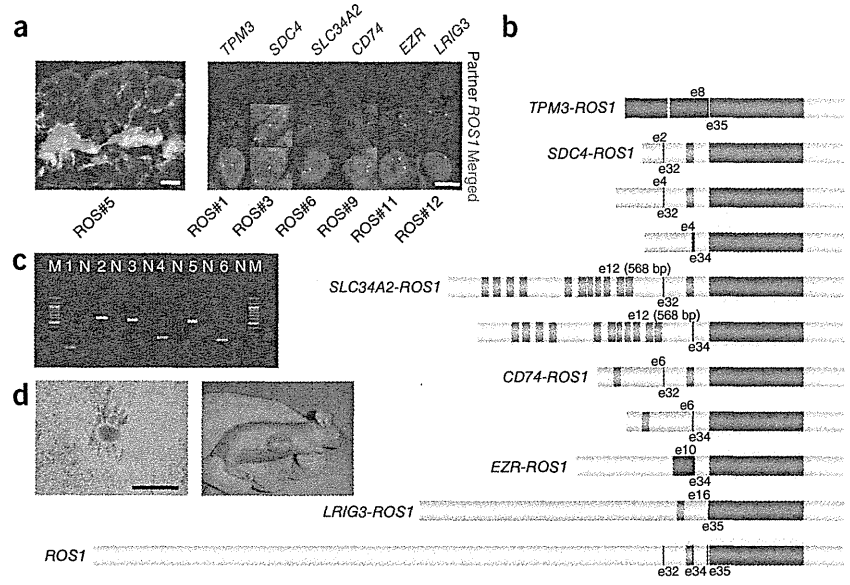

Figure 1 Identification of ROS1 fusions. (**a**) *ROS1* split (left) and fusion (right) FISH assay data (scale bars, 20 μm). In the split assay, multiple tumor cells harbored individual 3′ side signals (green), indicating the presence of a *ROS1* rearrangement. In the fusion assay, a fusion signal (yellow) was observed in the representative tumor cell of each subject, which is consistent with the presence of t(1;6)(q21.2;q22) for *TPM3-ROS1*, t(6;20)(q22;q12) for *SDC4-ROS1*, t(4;6)(q15.2;q22) for *SLC34A2-ROS1*, t(5;6)(q32;q22) for *CD74-ROS1*, inv(6)(q22q25.3) for *EZR-ROS1* or t(6;12)(q22;q14.1) for *LRIG3-ROS1*. (**b**) The break points of ROS1 are exons 32, 34 and 35. All of the break points allow the resulting fusion to harbor the kinase domain of ROS1 (red), and the exon 32 break point allows the resulting fusion to harbor the transmembrane domain of ROS1 (orange). In the fusion partners, dark blue and orange represent coiled-coil and transmembrane domains, respectively. Coiled-coil domains may contribute to homodimelization, but only TPM3 and EZR contained these domains. In contrast to ALK and RET fusions, the role of the fusion partner's coiled-coil domain is unknown in ROS1 fusions. e, exon. (**c**) Results for fusion-specific RT-PCR for tumors ROS#1 (lane 1, TPM3-ROS1, T8;R35, predicted product size of 119 bp), ROS#3 (lane 2, SDC4-ROS1, S2;R32, 596 bp), ROS#6 (lane 3, SLC34A2-ROS1, S13del2046;R32 and S13del2046;R34, 544 bp and 235 bp, respectively), ROS#8 (lane 4, CD74-ROS1, C6;R34, 230 bp), ROS#10 (lane 5, EZR-ROS1, E10;R34, 527 bp), and ROS#12 (lane 6, LRIG3-ROS1, L16;R35, 218 bp). M and N represent the size marker (100-bp ladder) and the non-template control, respectively. (**d**) The transforming potential of the ROS1 fusion. Mouse 3T3 fibroblasts infected with a retrovirus encoding SDC4-ROS1 derived from tumor ROS#4 formed multiple foci (scale bar, 1 mm). All of the four nude mice injected with the corresponding 3T3 cells developed a subcutaneous tumor (right).

(tumor RET#11). *RET* split FISH on the tissue arrays identified 22 fusion-positive tumors in 1,528 lung cancers (**Fig. 2a**), from which a multiplex RT-PCR system that captures all possible *KIF5B-RET* fusions detected 12 fusion-positive tumors: eight tumors with the fusion of *KIF5B* exon 15 and *RET* exon 12 (K15;R12) and one tumor each with the K16;R12, K22;R12, K23;R12 and K24;R11 fusions (**Fig. 2b** and **Supplementary Table 1**). The *KIF5B-RET* fusion FISH results were consistent with the presence of inv(10)(p11.22q11.2) in all 12 of these tumors (**Fig. 2a**).

In a routine histopathological diagnosis, we encountered an adenocarcinoma that showed a mucinous cribriform pattern (**Fig. 2c**) that was previously reported as a histopathological marker for the presence of EML4-ALK (**Supplementary Fig. 4**)[9–11]. Notably, this adenocarcinoma (tumor RET#14) was negative for ALK fusion and was positive for *CCDC6-RET*, as determined by FISH and inverse RT-PCR; the latter fusion gene was first described in thyroid cancer[12]. RT-PCR identified another tumor positive for the *CCDC6-RET* fusion (RET#13) in the remaining 10 tumors. The 14 RET-positive tumors (out of the total 1,528 tumors tested, with one additional tumor (RET#14) found through routine pathology diagnostic service) were also positive in the revised multiplex RT-PCR that captured *EML4-ALK*, *KIF5B-ALK*, *KIF5B-RET* and *CCDC6-RET* simultaneously (**Fig. 2d**). The RET kinase domain expression using real-time RT-PCR was weak or undetectable for the remaining nine tumors determined to be positive in the *RET* split FISH screening. Perhaps the genomic rearrangement occurred downstream of the *RET* break points. *RET* split FISH screening failed in three NSCLCs, including two adenocarcinomas. RET#14 was the index case found in routine pathology diagnostic service but not in the 1,528 cohort. RET fusions existed in 0.9% (13 out of 1,482) of the NSCLCs and 1.2% (13 out of 1,119) of the adenocarcinomas. The 14 RET fusion-positive subjects did not receive vandetanib.

We concluded that the rearrangements described above are somatic without using any matched normal tissues. Our histopathology-based screening method preserves the samples' histological architecture. This allows observers to confirm that internal non-tumor cells, for example, epithelial cells, inflammatory cells or fibroblasts, are negative in a test of interest.

All 71 kinase-fusion–positive (44 ALK, 13 ROS1 and 14 RET fusions) lung cancers were exclusively adenocarcinomas (6% of all adenocarcinomas in the present study), were positive for antibodies to TTF1, which is regarded as a marker for lung adenocarcinoma, as determined by immunohistochemistry (excluding two ALK-positive tumors) and were negative for *EGFR* and *KRAS* mutations. Thirteen of the 44 ALK-positive tumors (30%) were weakly positive for p63 expression (were weakly positive for a squamous cell carcinoma marker, p63) (**Supplementary Table 1**). Thirty-three tumors showed a mucinous cribriform pattern in at least 5% of their area; 22 tumors had this pattern in >25% of their area (**Fig. 2c**, **Supplementary Table 1** and **Supplementary Fig. 4**). The frequency of mucinous cribriform carcinoma was significantly higher in the kinase-fusion–positive group of tumors than in the 77 fusion-negative adenocarcinomas (22 out of 71 compared to 7 out of 77, respectively; $P = 0.00088$). Notably, we observed this pattern preferentially in EML4-ALK–positive tumors (70%, 29 out of 41); all three CD74-ROS1–positive tumors also showed this pattern. Recognizing this pattern in routine pathology diagnoses led to the identification of the CCDC6-RET fusion (tumor RET#14). In organs other than the lung, secretory breast carcinoma, which is characterized by a cribriform pattern with abundant secretory material, harbors the ets variant 6 (ETV6)-neurotrophic tyrosine kinase, receptor, type 3 (NTRK3) fusion (ref. 13). We identified an ALK-fusion–positive renal cell carcinoma that showed a mucinous cribriform pattern[7]. This pattern may be linked to the presence of particular kinase fusions[10], and this possibility warrants further study.

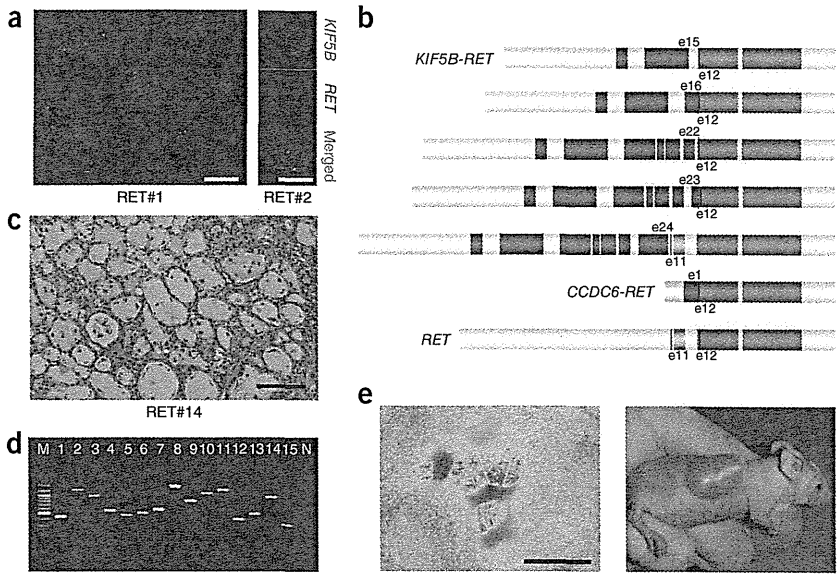

Figure 2 Discovery of RET fusions. (**a**) *RET* split (left) and fusion (right) FISH assay data (scale bars, 20 μm). In the split assay, multiple tumor cells harbored individual 3′ side signals (green), indicating the presence of *RET* rearrangement. In the fusion assay, a fusion signal (yellow) was observed in the representative tumor cell of subject RET#2, which is consistent with the presence of inv(10)(p11.22q11.2). (**b**) The break points of RET are exons 11 and 12. Both of the break points allow the resulting fusion to harbor the kinase domain of RET (red), and the exon 11 break point allows the resulting fusion to harbor the transmembrane domain of RET (orange). In the fusion partners, dark blue represents a coiled-coil domain, which probably contributes to the homodimelization of the fusion. Only the longer isoforms of RET and the RET fusions are shown. (**c**) Subject RET#14 showed the representative histopathology of mucinous cribriform carcinoma (scale bar, 100 μm). (**d**) The results for fusion-specific RT-PCR for subjects ALK#10 (lane 1, EML4-ALK, E13;A20, predicted product size of 432 bp), ALK#16 (lane 2, EML4-ALK, E20;A20, 1185 bp), ALK#26 (lane 3, EML4-ALK, E6;A20, 913 bp), ALK#38 (lane 4, EML4-ALK, E14;ins11del49A20, 546 bp), ALK#39 (lane 5, EML4-ALK, E2;A20, 454 bp), ALK#40 (lane 6, EML4-ALK, E13;ins69A20, 501 bp), ALK#41 (lane 7, EML4-ALK, E14;del14A20, 570 bp), ALK#42 (lane 8, KIF5B-ALK, K17;A20, 1,483 bp), ALK#44 (lane 9, KIF5B-ALK, K24;A20, 814 bp), RET#6 (lane 10, KIF5B-RET, K15;R12, 1,104 bp), RET#9 (lane 11, KIF5B-RET, K16;R12, 1,293 bp), RET#10 (lane 12, KIF5B-RET, K22;R12, 420 bp), RET#11 (lane 13, KIF5B-RET, K23;R12, 525 bp), RET#12 (lane 14, KIF5B-RET, K24;R11, 999 bp) and RET#13 (lane 15, CCDC6-RET, C1;R12, 352 bp). M and N represent the size marker (100-bp ladder) and non-template control, respectively. (**e**) The transforming potential of the KIF5B-RET fusion. Mouse 3T3 fibroblasts infected with a retrovirus encoding K15;R12L derived from tumor RET#7 fomed multiple foci (scale bar, 1 mm). All of the four nude mice injected with the corresponding 3T3 cells developed a subcutaneous tumor (right).

Supplementary Tables 1–4 summarize the clinicopathological features of the subjects. Briefly, young age, low smoking index and small tumor size characterized the kinase-fusion–positive group of subjects (**Supplementary Table 2**). A multivariate analysis of the adenocarcinomas revealed four independent factors that were indicators of poor prognosis: age ≥50 years, male sex, high pathological stage and negative kinase-fusion status (**Supplementary Table 3**). There was no significant difference in overall survival between the kinase-positive and epidermal growth factor receptor (EGFR)-mutant groups (P = 0.32). **Supplementary Table 4** shows the clinicopathological features of the subjects stratified by each fusion.

The transforming ability of CCDC6-RET and all of the ALK fusions, excluding K17;A20, was shown previously[1–3,8,12]. 3T3 cells infected with a virus expressing K17;A20, tropomyosin 3 (TPM3)-ROS1, syndecan 4 (SDC4)-ROS1, SLC34A2-ROS1, CD74-ROS1, ezrin (EZR)-ROS1, leucine-rich repeats and immunoglobulin-like domains 3 (LRIG3) (transcript variant 2)-ROS1 or KIF5B-RET (with both the longer (RET51) and shorter (RET9) RET isoforms) led to multiple transformed foci formation in culture and in subcutaneous tumors in a nude mouse tumorigenicity assay (**Figs. 1d, 2e** and **Supplementary Fig. 5**).

To test whether vandetanib, an inhibitor of vascular endothelial growth factor receptor (VEGFR-2), VEGFR-3, EGFR and RET[14], might be effective for the treatment of RET-fusion–positive tumors, we induced Flag-tagged EML4-ALK (E13;A20) or KIF5B-RET (K15;R12L and K15;R12S) in Ba/F3 cells, which are dependent on interleukin-3 (IL-3) for growth. All transfected cells, including those without any kinase fusion, proliferated in the presence of IL-3, but only cells expressing E13;A20 or K15;R12L grew in the absence of IL-3 (**Supplementary Fig. 6a**). In the absence of IL-3, vandetanib inhibited the proliferation of cells expressing K15;R12L (**Supplementary Fig. 6c**) but not the proliferation of cells expressing E13;A20 (**Supplementary Fig. 6d**). Crizotinib was not effective in inhibiting the proliferation of Ba/F3 cells expressing K15;R12L (**Supplementary Fig. 7**).

In 1985, a 3T3 assay identified *RET* as a rearranged transforming gene[15]. RET fusions have been identified exclusively in papillary thyroid carcinoma and are more frequently observed in radiation-associated thyroid cancers (for example, in survivors of the Chernobyl accident[16], atomic bomb survivors[17] and post-radiation therapy patients[18]). Therefore, a retrospective comparison of RET fusions in individuals with lung cancer with and without a history of radiation exposure warrants further study. If a positive association is found between RET fusion and radiation exposure in these studies, it might be desirable for individuals with internal or therapeutic exposure to irradiation (for example, those individuals involved in the Fukushima accident) to be monitored prospectively for lung cancer as well as thyroid cancer.

In Japan, more than 40% of lung adenocarcinomas in younger individuals harbor EGFR mutations[19]. In this study, 16% (17 out of 107) of younger individuals (≤50 years of age) with adenocarcinoma harbored a kinase fusion. Collectively, as long as molecular target diagnoses are properly performed, >50% of the individuals with lung adenocarcinoma in this generation may benefit from treatment with corresponding kinase inhibitors. Integrated pathology-based screening techniques can also be used for the selection of individuals to receive this treatment[20]. The results of our study will facilitate the development of a molecular classification of lung adenocarcinomas that is closely related to both the pathogenesis and the treatment of disease. This study was approved by the Institutional Review Board of the Cancer Institute Hospital, and all subjects provided informed consent.

METHODS

Methods and any associated references are available in the online version of the paper at http://www.nature.com/naturemedicine/.

Note: Supplementary information is available on the Nature Medicine website.

ACKNOWLEDGMENTS

We thank M. Iwakoshi, K. Shiozawa, T. Kakita, H. Nagano and K. Nomura for their technical assistance and S. Sengoku for providing administrative assistance. This work was supported in part by Grants-in-Aid for Scientific Research from the Ministry of Education, Culture, Sports, Science and Technology of Japan, as well as by grants from the Japan Society for the Promotion of Science; the Ministry of Health, Labor and Welfare of Japan; the Vehicle Racing Commemorative Foundation of Japan; the Princess Takamatsu Cancer Research Fund; and the Uehara Memorial Foundation.

AUTHOR CONTRIBUTIONS

K.T. conceived of and led the entire project, designed the FISH probes, screened samples using FISH and immunohistochemistry, performed histopathological analyses, generated figures and tables and wrote the manuscript. M.S. performed functional analyses and generated the figures. Y.T. performed inverse RT-PCR and RACE experiments and their corresponding analyses. R.S. conducted statistical analyses. S.S. performed FISH and histopathological analyses. S.H. processed and analyzed the tissue microarrays and FISH screening and generated figures. R.A. processed the FISH probe library. W.H. made and analyzed the database and processed tissue microarrays. H.N., H.U., Y.S., S.O. and K.N. collected specimens and clinical information and were involved in planning the project. Y.L.C. conducted functional analyses. H.M. supervised the functional analyses and planned the project. Y.I. performed histopathological analyses and collected specimens. All authors participated in the discussion and interpretation of the data and the results.

COMPETING FINANCIAL INTERESTS

The authors declare no competing financial interests.

Published online at http://www.nature.com/naturemedicine/.
Reprints and permissions information is available online at http://www.nature.com/reprints/index.html.

1. Soda, M. *et al. Nature* **448**, 561–566 (2007).
2. Takeuchi, K. *et al. Clin. Cancer Res.* **14**, 6618–6624 (2008).
3. Takeuchi, K. *et al. Clin. Cancer Res.* **15**, 3143–3149 (2009).
4. Rikova, K. *et al. Cell* **131**, 1190–1203 (2007).
5. Takeuchi, K. *et al. Haematologica* **96**, 464–467 (2011).
6. Takeuchi, K. *et al. Clin. Cancer Res.* **17**, 3341–3348 (2011).
7. Sugawara, E. *et al. Cancer* published online, doi:10.1002/cncr.27391 (17 January 2012).
8. Choi, Y.L. *et al. Cancer Res.* **68**, 4971–4976 (2008).
9. Inamura, K. *et al. J. Thorac. Oncol.* **3**, 13–17 (2008).
10. Takeuchi, K. *Pathol. and Clin. Med.* **28**, 139–144 (2010).
11. Jokoji, R. *et al. J. Clin. Pathol.* **63**, 1066–1070 (2010).
12. Grieco, M. *et al. Cell* **60**, 557–563 (1990).
13. Tognon, C. *et al. Cancer Cell* **2**, 367–376 (2002).
14. Flanigan, J., Deshpande, H. & Gettinger, S. *Biologics* **4**, 237–243 (2010).
15. Takahashi, M., Ritz, J. & Cooper, G.M. *Cell* **42**, 581–588 (1985).
16. Ito, T. *et al. Lancet* **344**, 259 (1994).
17. Hamatani, K. *et al. Cancer Res.* **68**, 7176–7182 (2008).
18. Bounacer, A. *et al. Oncogene* **15**, 1263–1273 (1997).
19. Kosaka, T. *et al. Cancer Res.* **64**, 8919–8923 (2004).
20. Han, B. *et al. Cancer Res.* **68**, 7629–7637 (2008).

Original Article

Identification of Anaplastic Lymphoma Kinase Fusions in Renal Cancer

Large-Scale Immunohistochemical Screening by the Intercalated Antibody-Enhanced Polymer Method

Emiko Sugawara, MD[1,2]; Yuki Togashi, MS[1,3]; Naoto Kuroda, MD[4]; Seiji Sakata, MD, PhD[1]; Satoko Hatano, BS[1,3]; Reimi Asaka, BS[1,3]; Takeshi Yuasa, MD, PhD[5]; Junji Yonese, MD, PhD[5]; Masanobu Kitagawa, MD, PhD[2]; Hiroyuki Mano, MD, PhD[6,7]; Yuichi Ishikawa, MD, PhD[3]; and Kengo Takeuchi, MD, PhD[1,3]

BACKGROUND: Several promising molecular-targeted drugs are used for advanced renal cancers. However, complete remission is rarely achieved, because none of the drugs targets a key molecule that is specific to the cancer, or is associated with "oncogene addiction" (dependence on one or a few oncogenes for cell survival) of renal cancer. Recently, an anaplastic lymphoma kinase (ALK) fusion, vinculin-ALK, has been reported in pediatric renal cell carcinoma (RCC) cases who have a history of sickle cell trait. In this context, ALK inhibitor therapy would constitute a therapeutic advance, as has previously been demonstrated with lung cancer, inflammatory myofibroblastic tumors, and anaplastic large cell lymphomas. **METHODS:** Anti-ALK immunohistochemistry was used to screen 355 tumor tissues, using the intercalated antibody-enhanced polymer (iAEP) method. The cohort consisted of 255 clear cell RCCs, 32 papillary RCCs, 34 chromophobe RCCs, 6 collecting duct carcinomas, 10 unclassified RCCs, 6 sarcomatoid RCCs, and 12 other tumors. **RESULTS:** Two patients (36- and 53-year-old females) were positive for ALK as determined by iAEP immunohistochemistry. Using 5′-rapid amplification of complementary DNA ends, we detected *TPM3-ALK* and *EML4-ALK* in these tumors. The results of this study were confirmed by fluorescence in situ hybridization assays. The 2 ALK-positive RCCs were unclassified (mixed features of papillary, mucinous cribriform, and solid patterns with rhabdoid cells) and papillary subtype. They comprised 2.3% of non-clear cell RCCs (2 of 88) and 3.7% of non-clear cell and nonchromophobe RCCs (2 of 54). **CONCLUSIONS:** The results of this study indicate that ALK fusions also exist in adult RCC cases without uncommon backgrounds. These findings confirm the potential of ALK inhibitor therapy for selected cases of RCC. ***Cancer* 2012;000:000-000.** © *2012 American Cancer Society.*

KEYWORDS: anaplastic lymphoma kinase, molecular-targeted therapy, renal cell carcinoma, immunohistochemistry, intercalated antibody-enhanced polymer.

INTRODUCTION

Renal cancer is one of the major cancers. The incidence and mortality of cases are estimated at 273,518 and 116,368 in the world; 14,963 and 6957 in Japan; and 56,678 and 13,711 in the United States.[1] The 5-year survival rate of patients with localized disease is relatively good: 65% to 93% and 47% to 77% for stages 1 and 2, respectively.[2] For advanced renal cancers (34%-80% and 2%-20% 5-year survival rates in stages 3 and 4, respectively),[2] several molecular-targeted drugs have been recently approved by the US Food and Drug Administration. These drugs, which include sunitinib, sorafenib, temsirolimus, everolimus, bevacizumab, pazopanib, and axitinib, are promising. However, none of them targets a key molecule that is specific to the cancer, or is associated with "oncogene addiction" of renal cancer, namely, the dependence on one or a few oncogenes for maintenance of the malignant phenotype and cell survival.

Anaplastic lymphoma kinase (ALK) fusion is a potential vulnerability, an "Achilles' heel", of many types of human cancer, including lymphoma,[3,4] sarcoma,[5] and carcinoma.[6,7] Experimentally, lung adenocarcinomas developed in EML4-ALK (fusion of ALK with echinoderm microtubule–associated protein like 4) transgenic mice were successfully treated with an ALK inhibitor.[8] The ALK inhibitor crizotinib has recently been used in patients with lung cancer, inflammatory myofibroblastic tumors (IMTs), or anaplastic large cell lymphomas (ALCLs), which harbor various ALK fusions. The compound showed an 81% response rate in ALK-positive lung cancers defined by at least 2 diagnostic methods,[9,10] and a

Corresponding author: Kengo Takeuchi, MD, PhD, Pathology Project for Molecular Targets, The Cancer Institute, Japanese Foundation for Cancer Research, 3-8-31 Ariake, Koto, Tokyo 135-8550, Japan; Fax: (81) 3-3570-0230; kentakeuchi-tky@umin.net

[1]Pathology Project for Molecular Targets, The Cancer Institute, Japanese Foundation for Cancer Research, Tokyo, Japan; [2]Department of Comprehensive Pathology, Graduate School, Tokyo Medical and Dental University, Tokyo, Japan; [3]Division of Pathology, The Cancer Institute, Japanese Foundation for Cancer Research, Tokyo, Japan; [4]Department of Diagnostic Pathology, Kochi Red Cross Hospital, Kochi City, Kochi, Japan; [5]Department of Urology, The Cancer Institute Hospital, Japanese Foundation for Cancer Research, Tokyo, Japan; [6]Division of Functional Genomics, Jichi Medical University, Tochigi, Japan; [7]Department of Medical Genomics, Graduate School of Medicine, University of Tokyo, Tokyo, Japan

We thank Tomoyo Kakita, Keiko Shiozawa, and Motoyoshi Iwakoshi for their technical assistance, and Sayuri Sengoku for providing administrative assistance.

DOI: 10.1002/cncr.27391, **Received:** October 1, 2011; **Revised:** October 31, 2011; **Accepted:** November 10, 2011, **Published online** in Wiley Online Library (wileyonlinelibrary.com)

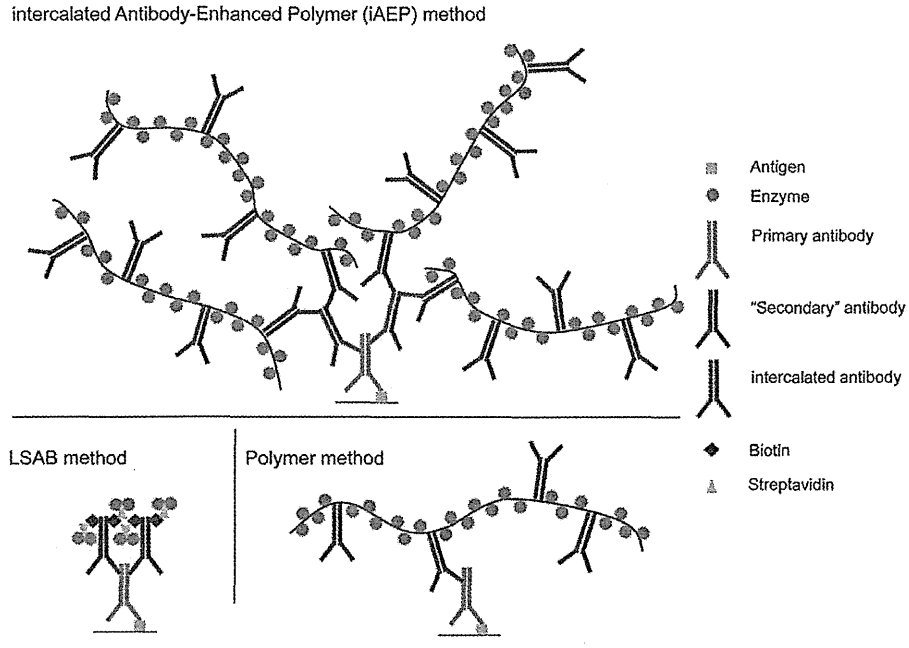

Figure 1. Schematic of intercalated antibody-enhanced polymer (iAEP) method is shown. The labeled streptavidin biotin (LSAB) and polymer methods are common conventional immunohistochemistry methods. In the iAEP method, a step of "intercalated antibody" is added between those of the primary antibody and polymer reagent. Thus, the iAEP method has an additional step compared with the polymer method, but the same number of steps as the LSAB method. There are generally 2 ways to raise the sensitivity of immunohistochemistry. The first is to raise the sensitivity of the antigen-antibody reaction, by increasing the concentration of the primary antibody, using a more sensitive antibody, antigen-retrieval technique, and so forth. The second is to raise the sensitivity of the detection system for the antigen-antibody immune complex. These 2 techniques may appear to generate the same result; however, in principle, they are totally different. The staining results are more likely to differ, especially when the antigen density is very low, such as for EML4-ALK (fusion of echinoderm microtubule-associated protein like 4 with anaplastic lymphoma kinase) or PPFIBP1-ALK (fusion of PTPRF interacting protein binding protein 1 with ALK).[13,24] In such a setting, the latter technique is more advantageous. The staining intensity depends on the density of enzyme in the antigen site. However sensitive a primary antibody is, the antigen-antibody complex cannot exceed the number of antigens. In contrast, it is easy to increase the enzyme density per antigen-antibody complex with use of the latter technique, which includes the iAEP method.

strong response in IMT for several months.[11] Two patients with ALCL who were receiving crizotinib achieved complete remission.[12] These findings indicate that ALK fusion addiction is one of the most promising targets in cancer therapy.

To ensure that such molecular-targeted therapy is effective and less toxic, accurate screening methods to detect ALK fusions are crucial. However, although immunohistochemistry has been a gold standard for the detection of ALK fusions in ALCL and IMT,[13,14] conventional anti-ALK immunohistochemistry is not sensitive enough to detect EML4-ALK, which was first described in lung cancer in 2007.[6,7] To overcome this, we developed a sensitive immunohistochemical tool, the intercalated antibody-enhanced polymer (iAEP) method (Fig. 1).[13] Combined with a conventional anti-ALK mouse monoclonal antibody 5A4, the iAEP method efficiently and consistently detected EML4-ALK in paraffin-embedded sections. In various studies on ALK-positive lung cancer, anti-ALK immunohistochemistry by iAEP or essentially equivalent methods was used to examine surgically resected specimens,[13,15-19] transbronchial lung biopsy specimens,[20] and endobronchial ultrasound-guided transbronchial needle aspiration specimens.[17,21,22] More importantly, some of the patients screened by anti-ALK iAEP immunohistochemical analysis received crizotinib therapy and showed a good response.[16,17,22] Novel ALK fusions, including v6 and v7 of EML4-ALK,[13] kinesin family member 5B (KIF5B)-ALK,[13] sequestosome 1 (SQSTM1)-ALK,[23] and PTPRF interacting protein, binding protein 1 (PPFIBP1)-ALK[24] have been identified using anti-ALK iAEP immunohistochemical analysis. Thus, anti-ALK iAEP immunohistochemistry constitutes a powerful tool for clinical and also research purposes.

The development of anti-ALK antibodies has facilitated the investigation of many types and cases of cancer, including lung cancer.[25-27] Since 1994, ALK-positive tumors have been identified exclusively in lymphoma

(ALCL and ALK-positive large B-cell lymphoma[28]) and sarcoma (IMT,[5] rhabdomyosarcoma,[26] and neuroblastoma[29]). It was not until 2007 that the presence of an ALK fusion was described in lung cancer.[6] This seems to be mainly because EML4-ALK is barely detectable by conventional anti-ALK immunohistochemistry. Considering in reverse, in cases of a tumor that is positive by anti-ALK iAEP immunohistochemistry, but negative by conventional anti-ALK immunohistochemistry, the tumor may have a novel ALK fusion partner, or express wild-type ALK at a modest level. Indeed, in "ALK-negative" IMT cases defined by conventional ALK immunohistochemistry, PPFIBP1-ALK was identified through reassessment for ALK fusions, using anti-ALK iAEP immunohistochemistry.[24] This prompted us to reevaluate other types of solid cancers for ALK fusions. Here, we describe the identification of TPM3-ALK (fusion of tropomyosin 3 and ALK) and EML4-ALK in renal cancer, by anti-ALK iAEP immunohistochemistry.

MATERIALS AND METHODS

Materials

We examined 355 renal tumor tissues from patients who had received surgery in the Cancer Institute Hospital, Japanese Foundation for Cancer Research, Tokyo, between 1994 and 2010. Renal tumors included 255 clear cell renal cell carcinomas (RCCs), 32 papillary RCCs, 34 chromophobe RCCs, 6 collecting duct carcinomas, 10 unclassified RCCs, 6 sarcomatoid RCCs, and 12 other tumors (4 oncocytomas, 3 angiomyolipomas, 1 solitary fibrous tumor, 2 spindle cell sarcomas, 1 desmoplastic sarcoma, and 1 anaplastic carcinoma). Surgically removed tumor specimens were routinely fixed in 20% neutralized formalin and embedded in paraffin for conventional histopathological examination. Immunohistochemical screenings were performed using tissue microarrays. For the 2 cases positive for anti-ALK immunohistochemistry, total RNA was extracted from the corresponding snap-frozen specimen, and purified with the use of an RNeasy Mini kit (Qiagen, Tokyo, Japan). Informed consent was obtained from the patients. The study was approved by the institutional review board of the Japanese Foundation for Cancer Research.

Immunohistochemistry

Formalin-fixed, paraffin-embedded tissue was sliced at a thickness of 4 μm, and the sections were placed on silane-coated slides. For antigen retrieval, the slides were heated for 45 minutes at 102°C in antigen retrieval solution (Nichirei Bioscience, Tokyo). For conventional immunostaining, the slides were incubated at room temperature with primary antibodies: ALK (5A4), vimentin, epithelial membrane antigen (EMA), cytokeratin 7, AE1/AE3, CAM5.2, 34βE12, α-methylacyl-coenzymeA racemase (AMACR), clusters of differentiation 10 (CD10), transcription termination factor 1 (TTF1), renal cell carcinoma marker (RCC Ma), paired box 2 (PAX2), and paired box 8 (PAX8) for 30 minutes. The immune complexes were then detected with polymer reagent (Histofine Simple Stain MAX PO; Nichirei Bioscience, Tokyo, Japan). For the sensitive detection of ALK fusion proteins, the ALK Detection Kit (Nichirei Bioscience), which is based on the iAEP method, was used.

Isolation of ALK Fusions

To obtain complementary DNA (cDNA) fragments corresponding to a novel ALK fusion gene, we used a 5′ rapid amplification of cDNA ends (5′-RACE) method with the SMARTer RACE cDNA Amplification Kit (Clontech, Takara Bio Inc., Shiga, Japan). We followed the manufacturer's instructions, with a minor modification: the ALK2458R primer (5′-GTAGTTGGGGTTGTAGTC GGTCATGATGGT-3′) was used as the gene-specific reverse primer. From the deoxythymidine oligomer–primed cDNA obtained from RNA from case 1, a 385–base pair (bp) cDNA fragment containing the fusion point was specifically amplified with the primers TPM3-705F (5′-AGAGACCCGTGCTGAGTTTGCTG-3′) and ALK3078RR (5′-ATCCAGTTCGTCCTGTTCA GAGC-3′). From case 2, a 454-bp cDNA fragment containing the fusion point was specifically amplified with the primers EML4-72F (5′-GTCAGCTCTTGAGT CACGAGTT-3′) and ALK3078RR. Polymerase chain reaction (PCR) analysis of genomic DNA for TPM3-ALK in case 1 was carried out with a pair of primers flanking the putative fusion point: TPM3-705F (5′-AGA GACCCGTGCTGAGTTTGCTG-3′) and Fusion-RT-AS (5′-TCTTGCCAGCAAAGCAGTAGTTGG-3′). For genomic PCR analysis of EML4-ALK in case 2, we used primers EML4-107F (5′-ATGAAATCACTGTGCTAA AGGCGGCT-3′) and Fusion-RT-AS (5′-TCTTGCCA GCAAAGCAGTAGTTGG-3′).

Fluorescence In Situ Hybridization

Fluorescence in situ hybridization (FISH) analysis of gene fusion was carried out with DNA probes for ALK, TPM3, EML4, and transcription factor E3 (TFE3). Unstained sections (4 μm thick) were subjected to hybridization with an ALK-split probe set (Dako, Tokyo, Japan), TFE3-split probe set (Kreatech, Amsterdam, The Netherlands), or bacterial artificial chromosome (BAC) clone-derived

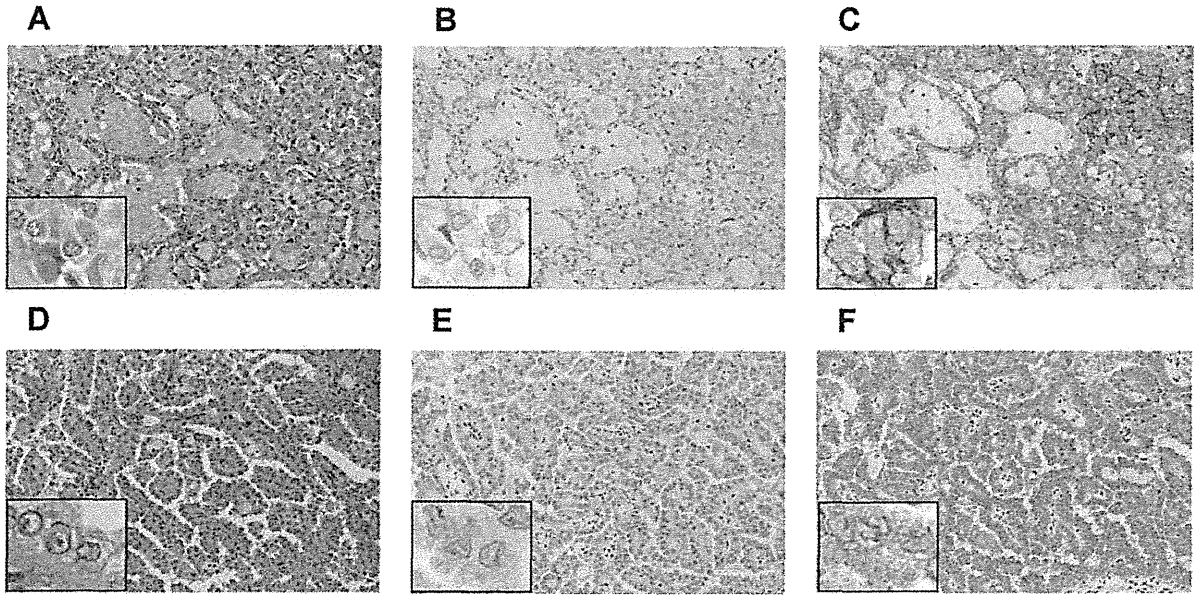

Figure 2. Histopathology of anaplastic lymphoma kinase (ALK)-positive renal cancer. Cuboidal tumor cells showed papillary, tubular, or cribriform growth patterns. The tumor cells had eosinophilic cytoplasm and round to ovoid nuclei. (A) The glandular structures possessed abundant mucin. (D) The tumor comprised a papillary structure of cuboidal or low columnar cells, with eosinophilic cytoplasm and small uniform round to oval nuclei (A,D hematoxylin and eosin stain). The tumor cells were (B) weakly positive and (E) indeterminate for ALK with conventional anti-ALK immunohistochemistry. (C,F) All of the tumor cells were clearly positive for ALK when the iAEP method was used. The staining pattern was diffuse cytoplasmic, with (C) membranous or (F) fine granular accentuation. Figures were taken using the corresponding whole sections (× 10 objective for low power view. × 40 objective for inset). Case 1 (A-C); Case 2 (D-F).

probes for ALK (RP11-984I21, RP11-62B19, RP11-701P18), TPM3 (RP11-809B24), and EML4 (RP11-996L7). Hybridized slides were then stained with 4′,6-diamidino-2-phenylindole and examined using a fluorescence microscope BX51 (Olympus, Tokyo, Japan).

Mutation Analyses for MET

A 1007-bp cDNA fragment containing the MET kinase domain was amplified using the primers MET-3186F (5′-GTCCATTACTGCAAAATACTGTCC-3′) and MET-4193R (5′-CACCTCATCATCAGCGTTATC-3′). The PCR product was sequenced after subcloning.

RESULTS

Identification of ALK Fusions in RCC Samples

Sections of tissue microarray were immunostained for ALK by the iAEP method, resulting in the detection of 2 positive cases (case 1, Fig. 2A-C; case 2, Fig. 2D-F). The positive results were also confirmed using corresponding whole histopathological sections, in which all of the tumor cells stained for ALK as other ALK-positive cancers usually do. We carried out 5′-RACE assays to determine whether these cases expressed ALK fusion or full-length ALK (mutated or unmutated). We isolated a cDNA fragment containing the exon 8 of *TPM3* fused in-frame to the exon 20 of *ALK* (Fig. 3A) in case 1, and the exon 2 of *EML4* fused to the exon 20 of *ALK* in case 2 (Fig. 3B). This EML4-ALK is called variant 5 (E2;A20) in lung cancer.[30] Reverse transcription PCR (RT-PCR) assays designed for the *TPM3-ALK* or E2;A20 successfully amplified cDNAs containing the fusion points (Fig. 3C,D). To confirm the genomic rearrangement, we performed FISH assays (Fig. 4) and genomic PCR (data not shown) for each fusion. All our results were consistent with the presence of t(1;2)(p21;p23)/*TPM3-ALK* in case 1, or inv(2)(p21p23)/E2;A20 in case 2. No other cases were positive for ALK by iAEP immunohistochemistry. All 355 cases were further examined by ALK-split FISH assay. In 12 of the cases, FISH was unsuccessful and not evaluable. In the other cases, the results were identical to those obtained by anti-ALK iAEP immunohistochemistry.

Case Presentation

Case 1

The patient was a 36-year-old woman who had a complaint suggestive of pyelonephritis. Magnetic resonance imaging and computed tomography showed a mass (4.0 cm × 4.0 cm × 3.5 cm) in the left kidney. No metastatic lesions or lymph node enlargements were identified. The patient had no past medical history of malignancy.

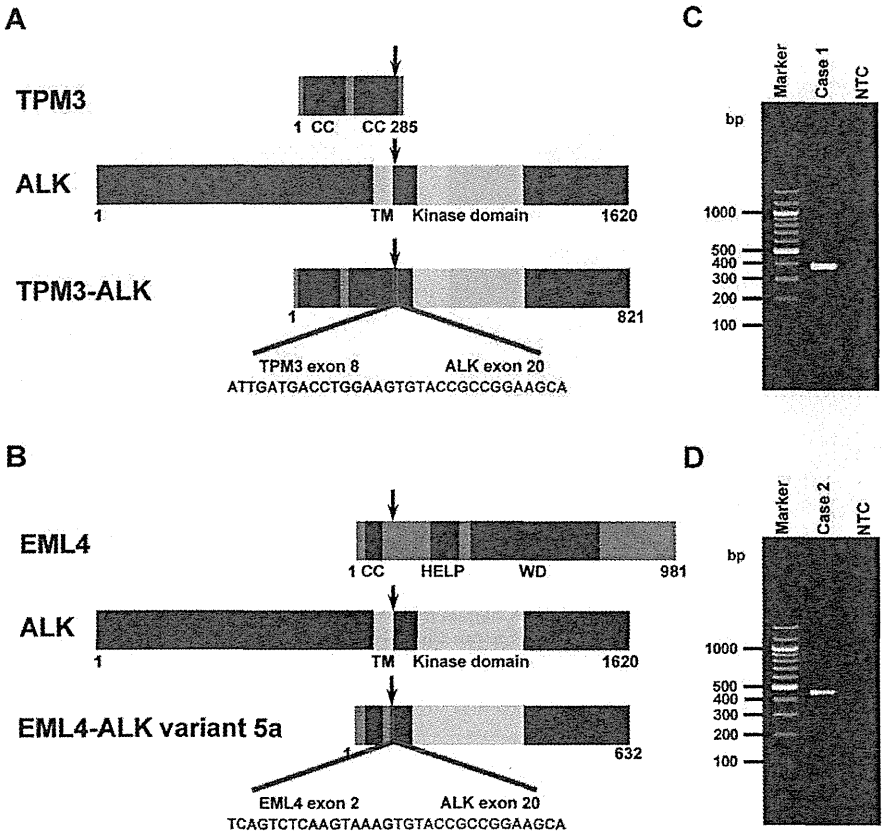

Figure 3. Identification of anaplastic lymphoma kinase (ALK) fusions. Tropomyosin 3 (TPM3) harbors 2 coiled-coil domains. (A) Case 1. A chromosome translocation generates a fusion protein in which the 2 coiled-coil domains of TPM3 and the intracellular region of ALK (containing the tyrosine kinase domain) are conserved. (B) Nucleotide sequencing of the polymerase chain reaction (PCR) products in case 2 revealed that exon 2 of echinoderm microtubule-associated protein like 4 (EML4), comprising a coiled-coil domain, was fused to exon 20 of ALK, generating the variant 5 complementary DNA (cDNA). In TPM3 and EML4 fusions, the region containing the coiled-coil domain is fused to the kinase domain of ALK. Numbers indicate amino acid positions of each protein. Arrow indicates the chromosomal breakpoint. The cDNA fragments of 385 base pairs (bp) and 454 bp were obtained by reverse transcription PCR, corresponding to (C) *TPM3-ALK* and (D) *EML4-ALK* variant 5, respectively. The left lane ("Marker") contains DNA size standards (100-bp ladder). CC indicates coiled-coil domain; HELP, hydrophobic echinoderm microtubule-associated protein; NTC, no-template control; TM, transmembrane domain; WD, WD repeats.

She underwent a translumbar left-radical nephrectomy and is currently alive and well without evidence of disease at 2 years of follow-up.

Case 2

A 53-year-old woman was found incidentally to have microscopic hematuria by medical check-up. Ultrasonography and magnetic resonance imaging showed a change in the left kidney, but the diagnosis was indefinite at that time. One year later, adenocarcinoma cells were detected by urinary cytology, and computed tomography revealed an isodence left renal mass (2.5 cm × 2.5 cm × 2.3 cm). The patient underwent a translumbar left-radical nephrectomy. She is currently alive and well at 7 years after surgery.

The patients had no episodes or family history indicative of sickle cell trait. To the best of our knowledge, there is no reported case of (genetically) Japanese individuals with sickle cell trait/disease.

Histopathological Examinations

The 2 ALK-positive renal cancers were papillary subtype and unclassified (with mixed features of papillary, mucinous cribriform, and solid patterns with rhabdoid cells). They comprised 2.3% of non–clear cell RCCs (2 of 88) and 3.7% of non–clear cell and nonchromophobe RCCs (2 of 54).

Case 1

Histologically, tumor cells were composed of papillary, tubular, or cribriform growth of cuboidal cells with

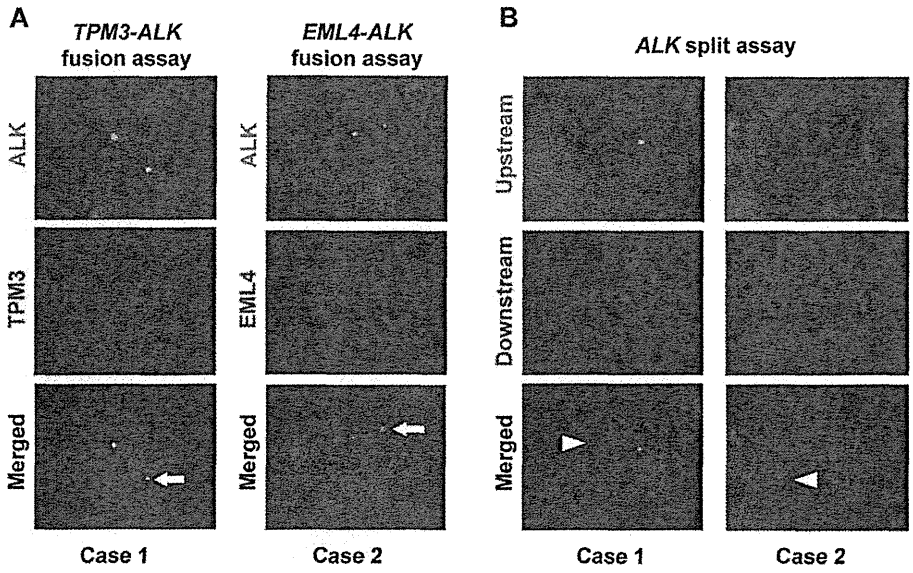

Figure 4. Fluorescence in situ hybridization analyses for *TPM3-ALK* (tropomyosin 3 fusion with anaplastic lymphoma kinase) and *EML4-ALK* (echinoderm microtubule-associated protein like 4 fusion with ALK). (A) In the *TPM3-ALK* and *EML4-ALK* fusion assays, the fusion genes are indicated by arrows. (B) The same clinical specimens as in (A) were subjected to fluorescence in situ hybridization analysis with differentially labeled probes for the upstream (green) or downstream (red) to the ALK breakpoint. In each case, the absence of 1 upstream signal indicated ALK rearrangement. Arrowhead indicates the rearranged ALK. The color of fluorescence for the bacterial artificial chromosome clones and the case numbers are indicated. Nuclei are stained blue with 4′,6-diamidino-2-phenylindole.

eosinophilic cytoplasm. The cribriform morphology consisted of tubular structures with flattened epithelial cells, compressed by mucinous pool and inter- or intracytoplasmic vacuoles. Solid sheets of tumor cells with occasional deeply eosinophilic intracytoplasmic inclusions and eccentric nuclei, resulting in rhabdoid features, were focally identified. Nuclei were round to ovoid, and the nuclear size was basically uniform. Irregular nuclear membranes and nuclear grooves were occasionally observed. Mitotic figures were scant. The background stroma in the tumor area possessed abundant mucin. Frequent deposition of psammoma bodies and infiltration of numerous foamy macrophages were also seen. A large amount of mucinous matrix was highlighted with Alcian blue stain. These histological features resembled the mucinous cribriform pattern frequently observed in ALK-positive lung adenocarcinoma,[18,31] and also a representative case of unclassified RCC by Lopez-Beltran et al,[32] favoring a diagnosis of unclassified RCC. Immunohistochemically, neoplastic cells showed a diffuse and strong positivity for ALK (iAEP), vimentin, EMA, cytokeratin 7, AE1/AE3, cytokeratin CAM5.2, and cytokeratin 34βE12, and focally staining for PAX2, PAX8, AMACR, and CD10. TTF1 and RCC Ma were completely negative. Intracytoplasmic inclusions corresponded to aggregates of intermediate filaments of vimentin. The ALK-staining pattern appeared to be accentuated around the cell membrane of rhabdoid cells. The MIB1 (mindbomb homolog 1) labeling index was less than 1%.

Case 2

Histologically, the tumor consisted of papillary configuration of cuboidal or low columnar cells, with eosinophilic cytoplasm and small uniform round to oval nuclei. A clear cell change was focally seen. Nuclei showed a round to oval shape, and nuclear grooves were frequently observed. The size variation of nuclei was minimal, and the irregularity of the nuclear membrane was evident. Nuclear pseudoinclusions were seldom seen. Small nucleoli were occasionally identified, but mitoses were absent. The fibrovascular cores of papillary architecture contained numerous psammoma bodies and foamy macrophages. In addition, glandular lumens of tumor cells focally contained myxoid materials. These findings morphologically corresponded to papillary RCC, but did not fit to types 1 and 2 by the classification of Delahunt and Eble.[33] In contrast, the features resembled papillary RCC, type 2A, described by Yang et al.[34] Alcian blue stain highlighted a small amount of stromal-type mucin. Upon immunohistochemical analysis, neoplastic cells were diffusely and